DANISH METEOROLOGICAL INSTITUTE

——— SCIENTIFIC REPORT ———

00-16

Towards an operational implementation of HIRLAM 3D-VAR at DMI

Kristian S. Mogensen, Jess U. Jørgensen
Bjarne Amstrup, Xiaohua Yang
and Xiang-Yu Huang

COPENHAGEN 2000

ISSN-Nr. 0905-3263 (printed)
ISSN Nr. 1399-1949 (online)
ISBN-Nr. 87-7478-426-9

Towards an operational implementation of HIRLAM 3D-VAR at DMI

Kristian S. Mogensen, Jess U. Jørgensen,
Bjarne Amstrup, Xiaohua Yang,
and Xiang-Yu Huang

Abstract

In this report we present results of the extensive testing of the HIRLAM 3D-VAR data assimilation system performed at DMI. We present results both for delayed mode runs and for pre-operational runs. In the delayed mode runs historical observations and ECMWF boundary data were used while in the pre-operational runs operational observations and ECMWF boundary data were used. In both cases the runs based on the HIRLAM 3D-VAR assimilation scheme were compared with similar runs based on the operational DMI-HIRLAM optimum interpolation (OI) assimilation scheme.

In both the delayed mode runs and the pre-operational runs the 3D-VAR based system gave similar or better verification scores compared to the OI based system. The additional computational cost of running 3D-VAR instead of running OI was roughly a factor of 2.3 per analysis. During all the runs the 3D-VAR system showed excellent stability with no crash.

Based on these results we argue that the HIRLAM 3D-VAR system now has reached a standard where it can be made operational.

1 Introduction

The goal of the HIRLAM (HIgh Resolution Limited Area Model) project is to make a complete numerical weather prediction system which enables the member countries to make high accuracy short range (up to about 48 hours ahead) operational weather forecasts. In order to produce accurate numerical weather forecasts both a good assimilation system and a good forecast model are needed.

The development of a variational data assimilation system within the HIRLAM community has been ongoing for several years now (Gustafsson *et al.*, 1999). The long term

goal of this part of the HIRLAM project is to produce a 4 dimensional variational data assimilation system (4D-VAR) which is capable of assimilating both conventional and new types of observation data, such as radar and satellite data.

An important milestone in the development of the HIRLAM variational data assimilation system is to have a working three dimensional variational data assimilation system (3D-VAR), which can produce good analyses (compared to the current HIRLAM reference optimum interpolation (OI) analysis system) with conventional observations. From this milestone, the development will continue into a 4D-VAR system with the capability of assimilation of new data types such as TOVS/ATOVS radiances and scatterometer winds etc.

Previously two comparisons between forecasts based OI and 3D-VAR analyses in delayed mode have been made consisting of a winter case by SMHI staff on the Cray T3E located at NSC Linköbing and a summer case by DMI staff on the Fujitsu VPP/700 located at ECMWF Reading. As reported in Lindskog *et al.*, (2000), better or comparable observation verification scores for 3D-VAR runs compared to OI runs were obtained. Based on these results we trust that the HIRLAM 3D-VAR system now has reached this milestone.

Before the 3D-VAR system can be used operationally, we need to test it in near operational conditions to ensure that the system can run on the operational computer (in DMI's case a NEC SX/4) and can handle the operational observational data and lateral boundaries.

In this report we present results for a more than 2 month long period of delayed mode parallel runs between the current operational OI assimilation system of DMI and the HIRLAM 3D-VAR assimilation system. In addition we present the results of two months of pre-operational runs with the HIRLAM 3D-VAR system. The experiments were performed on the NEC SX/4 computer at DMI.

The contents of the remainder of this report are as follows:

Overview of the HIRLAM 3D-VAR system briefly describes the HIRLAM 3D-VAR system. For a more complete description of the HIRLAM 3D-VAR system see Gustafsson *et al.*,(1999).

Main differences between HIRLAM optimum interpolation and 3D-VAR briefly outlines some of the differences between HIRLAM OI and 3D-VAR.

Experimental set-up describes the set-up used for both the delayed mode comparisons and the pre-operational comparisons.

Results presents the results in form of

Observation verification showing both daily and average scores when verifying against observations.

Field verification showing the average scores when verifying against analyses.

Subjective verification of storm cases where the performance of the HIRLAM 3D-VAR system is compared to the HIRLAM-OI system for the severe storms in December 1999.

Conclusions summarizes the results and discusses the possibility of an operational implementation.

2 Overview of the HIRLAM 3D-VAR system

The HIRLAM 3D-VAR data assimilation system consists of three major parts: 1) observation handling, 2) analysis and 3) diagnostics of the analysis. An overview figure of the system is given in Figure 1. The figure will be discussed in the relevant subsections below.

2.1 External observation handling for HIRLAM 3D-VAR

In the following we divide the discussion of observation handling into two parts: 1) external observation handling, which contains all data preprocessing and 2) internal observation handling within the assimilation cycle.

In the current 3D-VAR system observational data are converted from BUFR (WMO, 1995; Dragosavac, 1994) to central-memory array (CMA) (ECMWF, 1999). This data format has also been used by ECMWF & Meteo-France for the IFS/ARPEGE models. The primary development has been done at ECMWF and Meteo-France. The data format is described in detail in the manual (ECMWF, 1999). The conversion of BUFR to CMA is done in the step labeled *MAKECMA* on figure 1. The software used for this conversion is the same as the software used by ECMWF and Meteo-France with a few HIRLAM specific changes such as modified observation errors compared to ECMWF and support for ground based GPS data.

The CMA data format is based on encoding of all data into IEEE 64 bit floating-points. Integers and characters are encoded into the mantissa of the floating point data. The data format is intended to be optimized for computational speed rather than for efficient storage.

In the conversion from BUFR to CMA, the observational BUFR data is read report by report and checked against observation type and geographical location. If a report fits the selected observation types and geographical area, it is converted into a CMA report. The

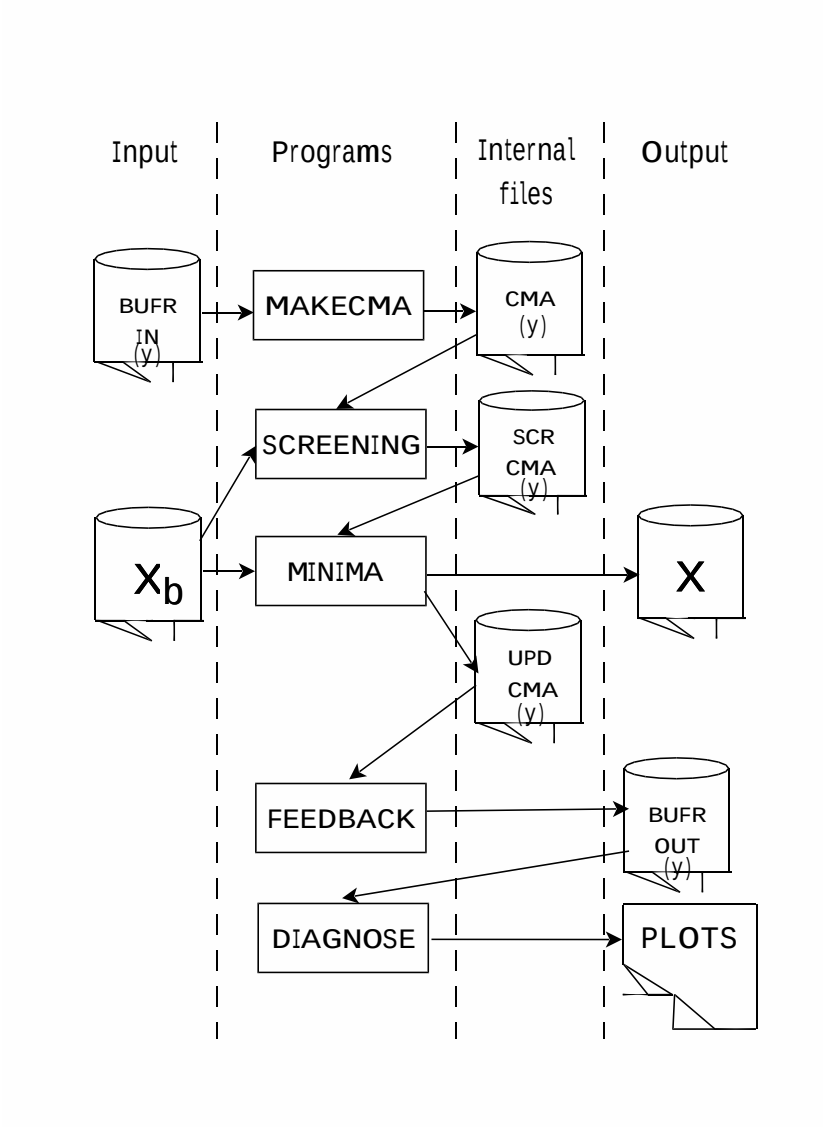

Figure 1: HIRLAM 3D-VAR program flow.

CMA report is written to a file containing two data description records (DDR's) with information about the processing date/time and number of observations of each type. This file is later used in the assimilation run.

In each CMA report space is allocated to store the difference between the background (either a 3 hour or a 6 hour forecast) and the observation and the difference between the analyzed value and the observation, which are calculated during the analysis. Before the analysis, these slots are initialized to zero.

2.2 3D-VAR analysis

The 3D-VAR analysis is based on the minimization of a cost function defined by the following equation (Lorenc, 1986)

$$J = J_B + J_o = \frac{1}{2}\delta\mathbf{x}^T\mathbf{B}^{-1}\delta\mathbf{x} + \frac{1}{2}\left(H\mathbf{x^b} + \mathbf{H}\delta\mathbf{x}^T - \mathbf{y}\right)^T\mathbf{R}^{-1}\left(H\mathbf{x^b} + \mathbf{H}\delta\mathbf{x}^T - \mathbf{y}\right) \quad (1)$$

where $\mathbf{x^b}$ is the background state (the first guess), $\delta\mathbf{x} = \mathbf{x} - \mathbf{x^b}$ is the analysis increment in form of the difference between the model state ($\mathbf{x}$) and the background state, $\mathbf{B}$ is the background error covariance matrix, H is the observation operator, $\mathbf{H}$ is the linearized observation operator, $\mathbf{y}$ is the observation vector, $\mathbf{R}$ is the observation error covariance matrix, and $()^T$ denotes the transpose. In the HIRLAM 3D-VAR formulation the model state is given by

$$\mathbf{x} = \begin{pmatrix} \mathbf{u} \\ \mathbf{v} \\ \mathbf{T} \\ \mathbf{q} \\ \ln \mathbf{p_s} \end{pmatrix}. \quad (2)$$

To avoid the inverse of $\mathbf{B}$ and impose balance among variables the following transform is applied:

$$\chi = \mathbf{PVLFS^{-1}AF^{-1}}\delta\mathbf{x} = \mathbf{U}\delta\mathbf{x} = \mathbf{U}(\mathbf{x} - \mathbf{x^b}) \quad (3)$$

where $\mathbf{F}$ is the Fourier transform to spectral space, $\mathbf{F^{-1}}$ is the inverse Fourier transform, $\mathbf{A}$ is the subtraction of the geostrophic wind increment from the full wind increment, $\mathbf{S^{-1}}$ is the normalization with the forecast error standard deviation, $\mathbf{L}$ is the normalization by the square-root of the spectral density of the horizontal forecast error correlation, $\mathbf{V}$ is the projection on the eigenvectors of the vertical forecast error correlation matrix, $\mathbf{P}$ is the normalization by the square root of the vertical eigenvalues and $\mathbf{U} = \mathbf{PVLFS^{-1}AF^{-1}}$. By this transform the cost function can be written as

$$J = J_b + J_o = \frac{1}{2}(\chi)^T(\chi) + \frac{1}{2}(H\mathbf{x^b} + \mathbf{HU^{-1}}\chi - \mathbf{y})^T\mathbf{R^{-1}}(H\mathbf{x^b} + \mathbf{HU^{-1}}\chi - \mathbf{y}) \quad (4)$$

which do not contain the above described inverse. For details concerning these transformations see Gustafsson *et al.*, (2000).

The 3D-VAR program reads the observations from a CMA file and a background field from a GRIB file (typically a 3 or 6 hour forecast, denoted as the $\mathbf{x^b}$ in Figure 1). Currently the following observations (with the information possible to use given after each observation type) are supported : SYNOP (pressure, 2 meter temperature, 2 meter relative humidity, 10 meter wind), SHIP (pressure, 2 meter temperature, 2 meter relative

humidity, 10 meter wind), DRIBU (pressure, 2 meter temperature, 2 meter relative humidity, 10 meter wind), AIREP/AMDAR/ACARS (temperature, wind), PILOT (wind), TEMP (temperature, wind, humidity) and SATOB (wind). Support for additional data types (*e.g.* (A)TOVS data) is currently under development.

When the observations and background have been read, the background ($\mathbf{x}^b$ in eq. 4) is transformed from grid-point space to observation space using the observation operators (H in eq. 4) and the difference between the background and the observations is calculated ($(H\mathbf{x^b} - \mathbf{y})$ in eq. 4). Since this term is constant for all values of χ it only needs to be evaluated once. The differences between the background and the observations are stored in the CMA data.

The observations are checked by a screening module (labeled *SCREENING* on Figure 1). The screening module does the following checks (details about the checks can be found in Gustafsson *et al.*,(1999)):

Bad reporting practice check to remove *e.g.* ships reporting over land.

Blacklist check to remove stations assumed not to produce correct data.

First guess check to remove observations too far from the first guess.

Multi-level check to remove multi-level observations with too many failed single level checks.

Redundancy check to remove redundant information *i.e.* dense reports from aircrafts.

Only observations which passes the screening checks are used in the minimization step. Labels specifying reasons for rejection of individual observations are stored in the CMA data (labeled *SCR CMA* in Figure 1).

To calculate the background constraint a file containing information about the structure of the background covariance matrix (the $\mathbf{B}$ matrix in eq. (1)) is read. The latter is calculated using the NMC method (for details see Berre, (1997) and Gustafsson *et al.*,(1999)).

In the minimization step (labeled MINIMA in Figure 1) an iterative procedure based on the gradient of the cost function (eq. (1)) is used (Gilbert and Lemaréchal, 1989). The number of iterations is determined by the required accuracy of the solution. There is no simple way to predict the number of iterations needed to acquire the requested accuracy, since it depends on the number of observations and the current weather situation. During each iteration of the minimization the difference between observation and current model state χ (given by $(H\mathbf{x^b} + \mathbf{HU^{-1}}\chi - \mathbf{y})$) is stored in the CMA data. The result of the

minimization is an analysis field (labeled **X** in figure 1) stored in a GRIB file. In addition, the differences between the observed and analyzed values at the observation points are stored in a CMA file (labeled *UPD CMA* in figure 1).

During the minimization it is possible to apply *variational quality control* of the observations. The details can be found in Andersson and Järvinen, (1999) and Gustafsson *et al.*, (1999). The idea of variational quality control is, that the cost function is modified in a way where observations which differ greatly from the current model state are given very little weight in calculation of the gradient of the cost function. In order to prevent rejection of correct observations by such a method, the variational quality control is switched on after some pre-determined iteration number (typically 20). If, during the minimization, the model state approaches an observed value of a rejected observation, the observation will start to influence the cost function again. Each observation is given a grade based on a 1 to 4 scale with

1. corresponding to a correct observation,
2. corresponding to a probably correct observation,
3. corresponding to a probably incorrect observation and
4. corresponding to an incorrect observation.

Afterwards it is possible to look at which observations are rejected by the variational quality control, since the information about the grade of each observation is stored in the CMA file.

The HIRLAM 3D-VAR system also contains a spectral version of the HIRLAM forecast code, since the calculation of the background constraint requires a lot of the same calculations as in the spectral HIRLAM forecast code. The spectral forecast code is also part of the HIRLAM 4D-VAR system which is presently in the process of development.

2.3 Diagnostics

In order to validate the performance of an assimilation system a good diagnostics tool is important to have. As mentioned above the updated CMA file contains necessary information which can be used to investigate the performance of the analysis system and to tune the parameters of the variational system.

Examples of such investigations/tuning could be

1. Continuous monitoring of stations which repeatedly fails either the screening or the variational quality control.

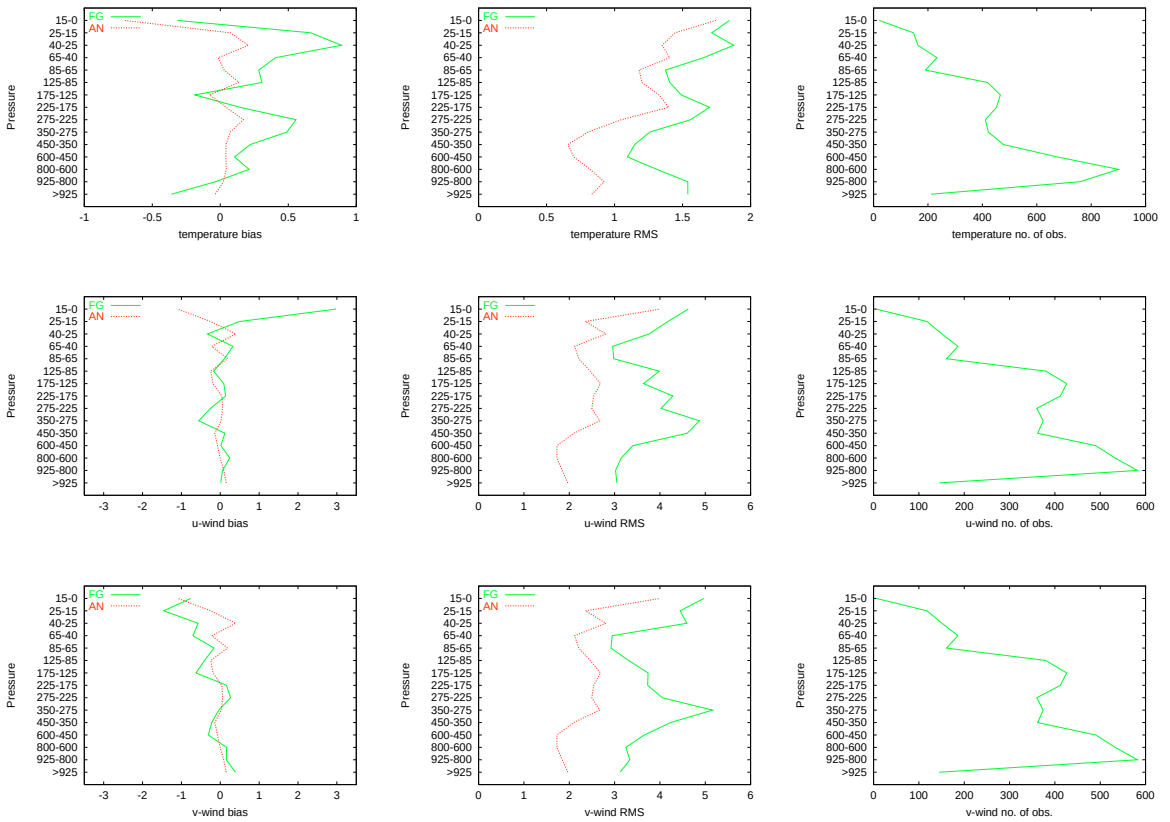

Figure 2: Example of a statistical evaluation of a 3D-VAR analysis valid on 1999120112.

2. Statistical evaluation of each individual 3D-VAR analysis.. An example of such calculations is given in Figure 2.

3. Production of maps showing the geographical dependency of screening decisions to investigate if the assimilation system has problems in *e.g.* areas of steep orography.

4. Recalculation of the observation errors using the method described by Hollingsworth and Lönnberg (Hollingsworth and Lönnberg, 1986; Lönnberg and Hollingsworth, 1986). This has previous been done for the HIRLAM 3D-VAR system (Lindskog *et al.*, 2000) but should probably be done regularly.

2.4 Parallelization issues of the HIRLAM 3D-VAR system

Most of the early development work of the HIRLAM 3D-VAR system including the spectral forecast model was done at SMHI on the CRAY T3E located at the National Supercomputer Centre in Linköbing. In the original implementation the code was parallelized using explicit message passing with the CRAY/SGI library SHMEM.

The code was ported to the FUJITSU VPP/700 in a non-parallel version. To increase performance by using multiple processors work commenced on porting the message passing using SHMEM to a more portable library in forms of the message passing interface (MPI) library. The advantage of using MPI is that this library is available on most (if not all) supercomputers. The work was done in a close collaboration between DMI and SMHI.

The internal observation handling of the 3D-VAR code is parallelized using the following two disjoint strategies:

LOCOB: In this strategy the domain is divided into a number (equal to the number of processors used for the execution) of sub-domains and the observations are distributed into the sub-domain after the geographical location of the observation. The advantage of such a strategy is that the background field at the observation point can by evaluated in the same processing element (PE) as the observation point, so no message passing of observation or background field is necessary. However, this strategy has the disadvantage that the load distribution is unequal due to irregular distribution of the observations.

NON-LOCOB: In this strategy observations are distributed evenly to all processors, and the background fields at the observation points are sent by message passing between the processing elements. This strategy has the advantage of an even load distribution of all processors. The disadvantage is that more message passing is needed compared with the LOCOB option.

It has previously been shown, that on a Cray T3E computer using the SHMEM library the NON-LOCOB option is the fastest one when running on many processors (Lindskog and Gustafsson, 1998). Similar tests on the NEC SX/4 on 1 to 8 processors showed little or no real differences in timing between the two strategies.

At ECMWF the external observation handling has been parallized using the ECMWF message passing (MP) parallel library (Saarinen, 2000). However this software has currently not parallelized in the HIRLAM 3D-VAR framework. Work on a parallel version of the observation handling within the HIRLAM framework is planned to start during the fall of the year 2000. It is however not clear if the benefit of a parallel version of the observation handling will be significant since for the input BUFR data to the DMI-HIRLAM-G the observation handling presently only takes around 1 minute. When it becomes possible to use satellite data in the 3D-VAR analysis, the amount of work in the observation processing will be greater, thereby requiring a parallel version of the observation processing.

3 Main differences between HIRLAM optimum interpolation and 3D-VAR

From a practical point of view the main differences between the current HIRLAM OI system and the present version of HIRLAM 3D-VAR can be summarizes as follows:

Realization of the analyse schemes: In the way the optimum interpolation is realized the domain is divided into a collection of observation boxes and the assimilation is done within each box whereas for the 3D-VAR analysis scheme the cost function is minimized over the whole domain.

Use of observations : For multilevel observations (*e.g.* radiosondes) the OI scheme uses a fixed number (15) of standard pressure levels whereas 3D-VAR uses all significant levels of each report. This difference could lead to better vertical structure of the 3D-VAR analyses compared to the OI analyses. The information used from some observations is also different in the 3D-VAR system compared to the OI system. An example of this is that the 3D-VAR system uses temperature and the OI system uses geopotential from radiosondes.

There are other small difference in *e.g.* how observations are screened, quality controlled *etc.*

In the future the use of new data types (some of them are difficult to use in OI) in the HIRLAM 3D-VAR system will add yet another important difference. The integration of these new data types into the HIRLAM 3D-VAR system is currently in the development stage. Based on the experiences at other centres (such as ECMWF and UKMO) this development could lead to significant improvement in the performance of the variational analysis.

4 Experimental set-up

The experimental set-up was constructed based on the operational HIRLAM set-up at DMI (Sass *et al.*, 1999).

4.1 Domain

The domain was the operational DMI-HIRLAM-G area consisting of 202 by 190 grid-points with 31 vertical levels with a horizontal resolution of 0.45 degrees (shown in Figure 3). This domain is on a rotated grid with polar coordinates $(P_{lat}, P_{lon} = (0.0°, 80.0°)$ starting at $(x_{lon,1}, y_{lat,1}) = (-63.725°, -37.527°)$ in the rotated coordinate system.

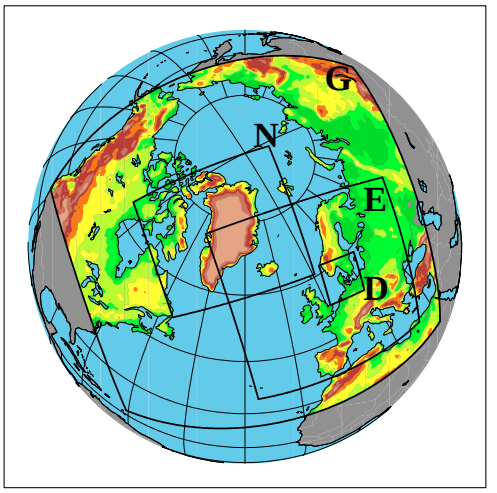

Figure 3: Operational DMI-HIRLAM areas.

4.2 Forecast model

The forecast model used was an updated version of the operational model described in Sass *et al.*, (1999). As for the operational DMI-HIRLAM-G model an Eulerian time stepping with a time step of 240 seconds was used with physics increment every third time step.

4.3 Observation types used

As in the operational set-up (Sass *et al.*, 1999) we used the following observation types: SYNOP, SHIP, DRIBU, PILOT, TEMP and AIREP (including AMDAR and ACARS) in all 3D-VAR and OI runs.

4.4 Set-up for delayed mode runs

For experiments a period from 20 October 1999 to 31 December 1999 was selected. This period covers both the last part of the EUCOS (EUMETNET Composite Observing System) special period with an extended set of AMDAR data (until 15 November) and the heavy storms of December 1999 (both over Denmark on 3 December and over France on 25 and 27/28 December).

The assimilation window was 6 hours (observation window $\pm$ 3 hours) centered around the main synoptic times (00Z, 06Z, 12Z and 18Z) with each assimilation cycle consisting of the following steps:

1. Observation preparation from BUFR data.

2. Assimilation.

3. Non-linear normal mode initialization.

4. A 48 hour forecast.

For lateral boundaries to the forecast model ECMWF analyses and 6 hour forecasts originating from 00Z and 12Z were used.

4.5 Set-up for pre-operational runs

In these experiments results with the current pre-operational forecast code was used for direct comparisons with other pre-operational tests based on OI. In the pre-operational set-up the runs were executed with similar conditions as the operational system, but with a delay, since the pre-operational tests were not time-critical.

In order to save computer time the first pre-operational 3D-VAR tests were performed with a six hour assimilation cycle instead of a three hour assimilation window as for the operational DMI-HIRLAM-G model. To ensure a fair comparison an additional OI experiment with six hour data assimilation cycle was performed.

As lateral boundaries ECMWF forecasts were used with a lateral boundary update every 6 hours.

As in the operational runs we applied a scheme which merges HIRLAM and ECMWF analyses two times a day. When the 00Z ECMWF analysis has arrived at DMI, it is combined with the corresponding HIRLAM analysis in a way which takes the large scales from the ECMWF analysis and the small scales from the HIRLAM analysis. This combined field is then used to produce a new first guess for the 06Z assimilation. A similar procedure is repeated with the 12Z ECMWF analysis. This scheme is based on the assumption that ECMWF analyses are of better quality than the corresponding HIRLAM analyses for large scales in particular over the Atlantic ocean.

The assumption that ECMWF analyses are of better quality than the corresponding HIRLAM analyses can be argued based on several factors such as a more advanced assimilation scheme (4D-VAR *versus* OI/3D-VAR), extensive use of satellite data (*e.g.* ATOVS data) and a longer cut-off for acceptance of observations in the ECMWF 4D-VAR. Indeed the use of this procedure has previously been tested and significantly better results were found for most cases compared to not using it.

The pre-operational runs were started in March 2000 and after solving some logistic problems and adjusting the configuration *etc.* stable and meaningful runs were achieved from mid-May and onwards. In this report results for the pre-operational runs covering June and July 2000 are presented.

5 Stability and computer time requirement of the HIRLAM 3D-VAR system

In all the runs presented in this report we have not had any problems with stability of the 3D-VAR code. Earlier we have had problems with the observation processing originating from having too small buffers in the BUFR decoding. Upgrading the observation processing software in mid-May solved the problems.

Typically, using four MPI processes on DMI's NEC SX/4, a 3D-VAR analysis with normal DMI input BUFR observations for the DMI-HIRLAM-G area (see above) takes around 10 minutes. This should be compared with 3 minutes for the current operational OI analysis system on four processors. Thus the 3D-VAR system is significantly more computational expensive compared to the OI system.

6 Results of delayed-mode runs

6.1 Observation verification against EWGLAM stations

For the delayed mode runs we have performed observation verification against EWGLAM stations for the following forecasted parameters: mean sea level pressure (Fig. 4), 2 meter temperature (Fig. 4), 10 meter wind (Fig. 4), geopotential height at 850 hPa, 500 hPa and 250 hPa (Fig. 4), temperature at 850 hPa, 500 hPa and 250 hPa (Fig. 5), wind at 850 hPa, 500 hPa and 250 hPa (Fig. 5) and relative humidity at 850 hPa and 500 hPa (Fig. 6). For the verification we have used ECMWF analyses to exclude questionable observations from the EWGLAM stations. In these figures averaged values over the whole period are presented.

Comparing the observation verification results (Figs. 4 to 6) the RMS values from 3D-VAR runs are better than those from OI runs for most parameters. In particular for high levels (250 hPa) the scores are significantly better for the 3D-VAR runs. The explanation for this is probably that the OI analysis is made on standard pressure levels and the 3D-VAR analysis is made on model levels taking all significant levels of *e.g.* radiosonde report into account. Also for lower levels the 3D-VAR run has slightly better RMS values than the OI run. Looking at the bias it seems that the 3D-VAR run has a higher bias in mean sea level pressure and in 850 hPa height and temperature. It has previously been discussed (Gustafsson *et al.*, 1999) that the current 3D-VAR formulation with analysis done on model levels and in spectral space may have problems near steep orography. We suspect that this problem has not been completely solved yet and more work needs to be

done.

6.2 Daily observation verification

In addition to time-averaged verification scores we have also calculated the daily standard deviation and bias for various parameters. Examples of such statistics for a forecast length of 24 hours are given in Fig. 7. From the figure it can be seen, that for most days the 3D-VAR and OI runs give very similar results. However for a few cases the OI runs have significantly higher standard deviations in mean sea level pressure compared to the 3D-VAR runs. The number of such forecast failures are somewhat less in the 3D-VAR runs. latter.

6.3 Observation verification against Danish and Greenlandic stations

Since DMI's primary responsibility is to produce good forecasts for Denmark, Greenland and the Faeroe Islands we have paid special attention to the observation verifications against Danish and Greenlandic stations. The results are shown on Fig. 8. RMS values for mean sea level pressure are clearly lower for the 3D-VAR runs compared with the OI runs. The bias for mean sea level pressure is higher for the 3D-VAR runs for the verification against Greenlandic stations, but not for Danish stations. We suspect that this is caused by the treatment of 3D-VAR for the steep orography of Greenland, as has been discussed in 6.1.

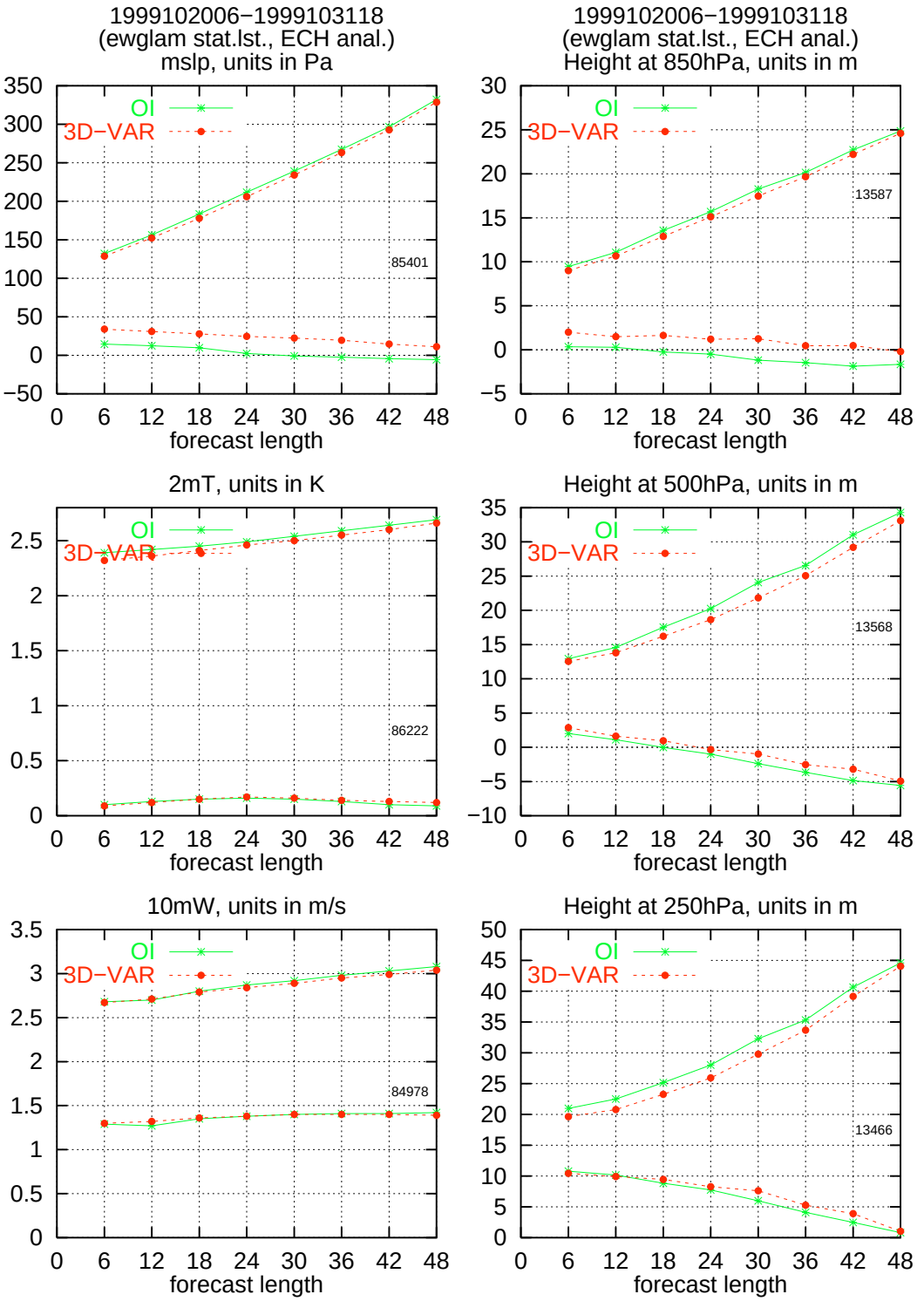

Figure 4: Observation verification scores (bias and RMS) against EWGLAM stations for mean sea level pressure, 2 meter temperature, 10 meter wind, and height at 850 hPa, 500 hPa, and 250 hPa for the period the experiments covering 1999102006 to 1999123118.

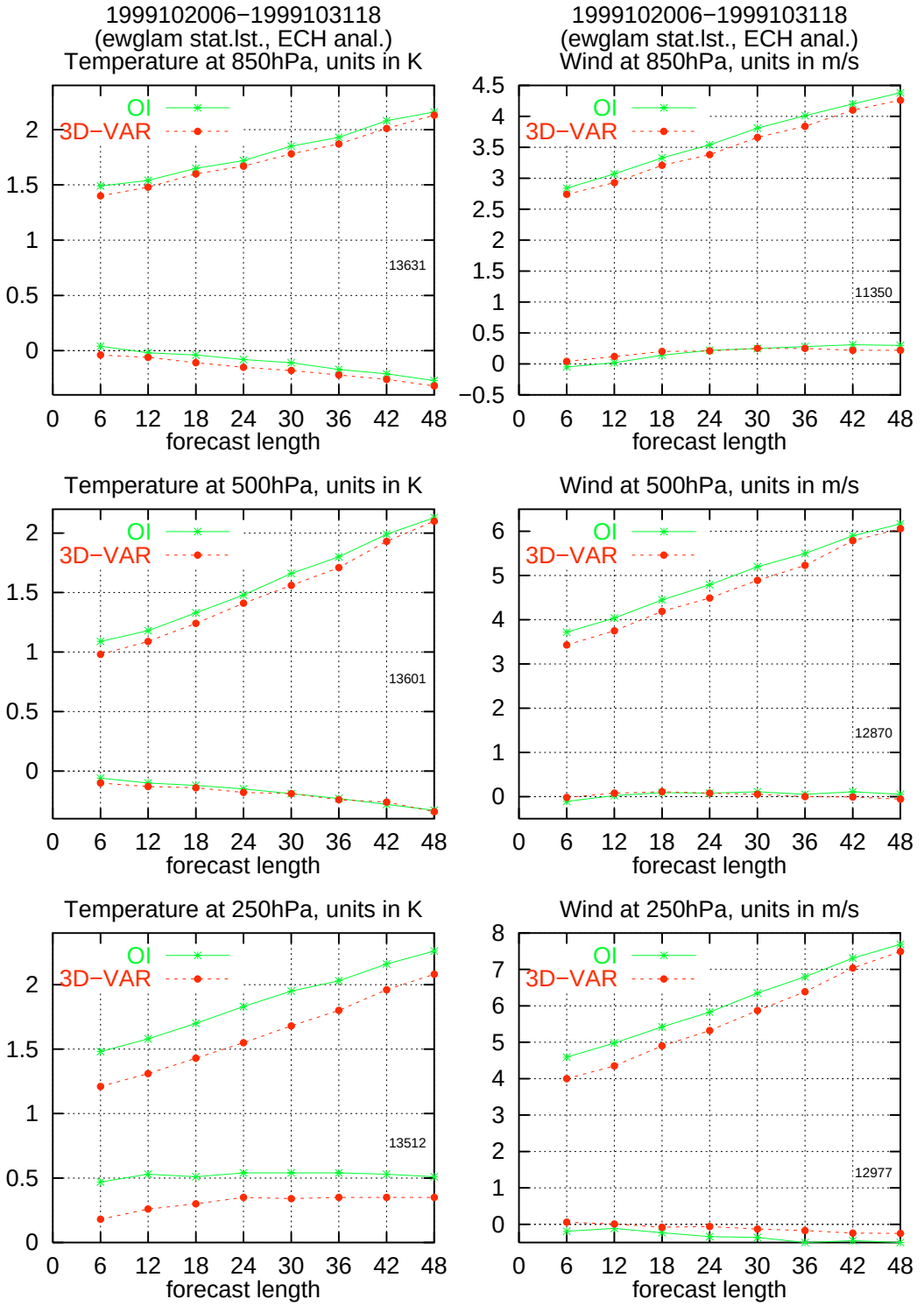

Figure 5: Same as in Fig. 4 but for temperature and wind at 850 hPa, 500 hPa, and 250 hPa.

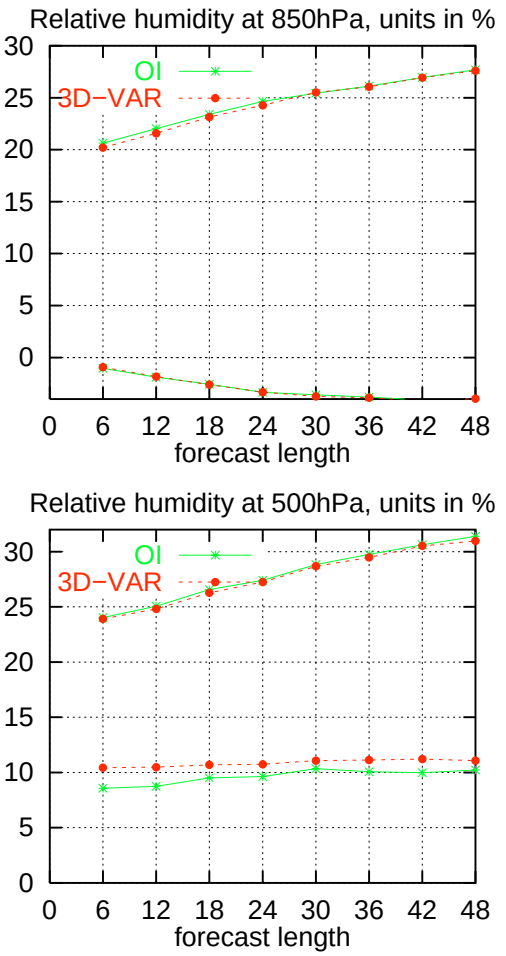

Figure 6: Same as in Fig. 4 but for relative humidity at 850 hPa, and 500 hPa.

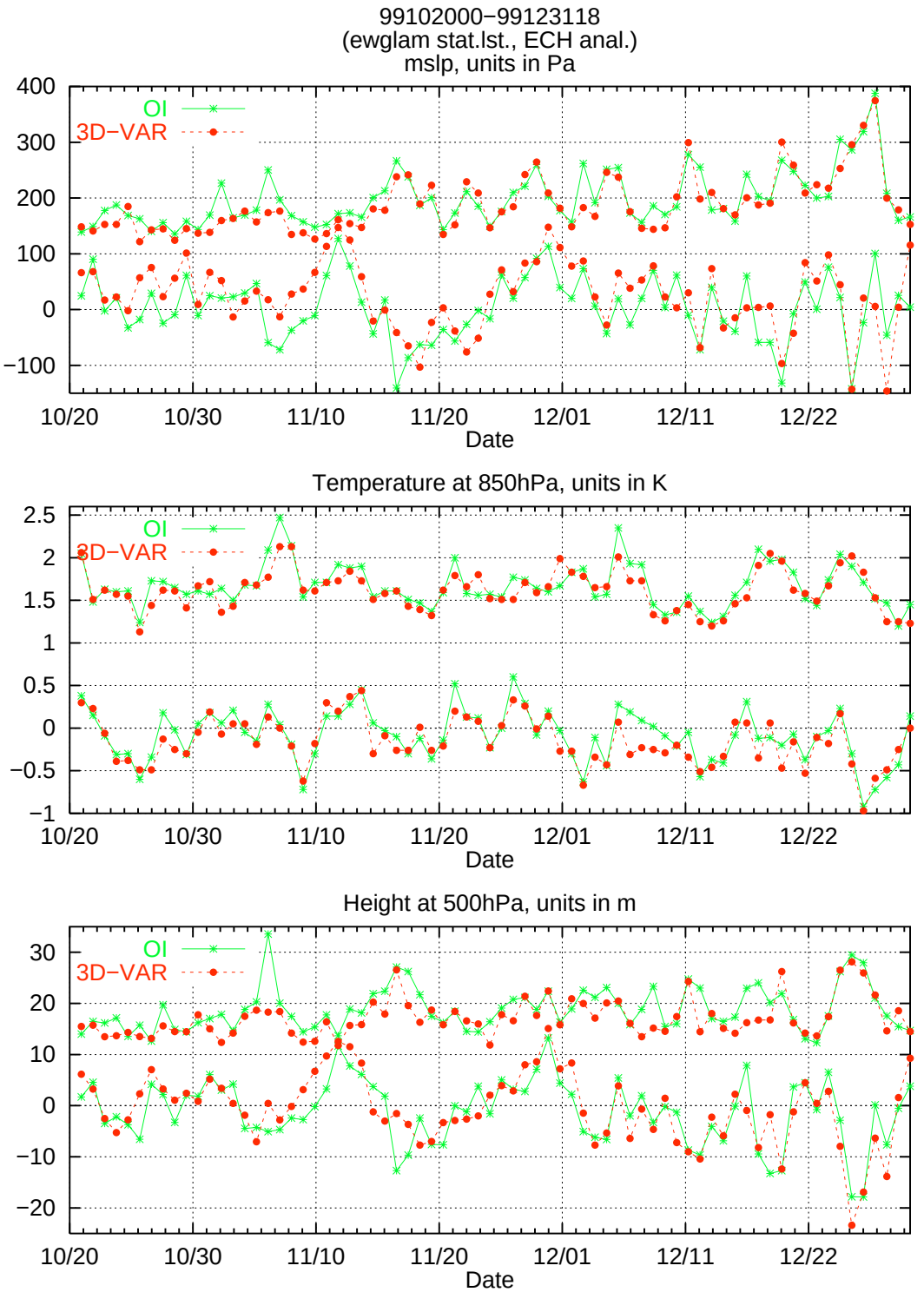

Figure 7: Daily observation verification (standard deviation and bias) for 24 hour forecasts for mean sea level pressure, 850 hPa temperature and 500 hPa geopotential height against EWGLAM stations. The date indicated on the x-axis is the valid date for the 24 hour forecasts.

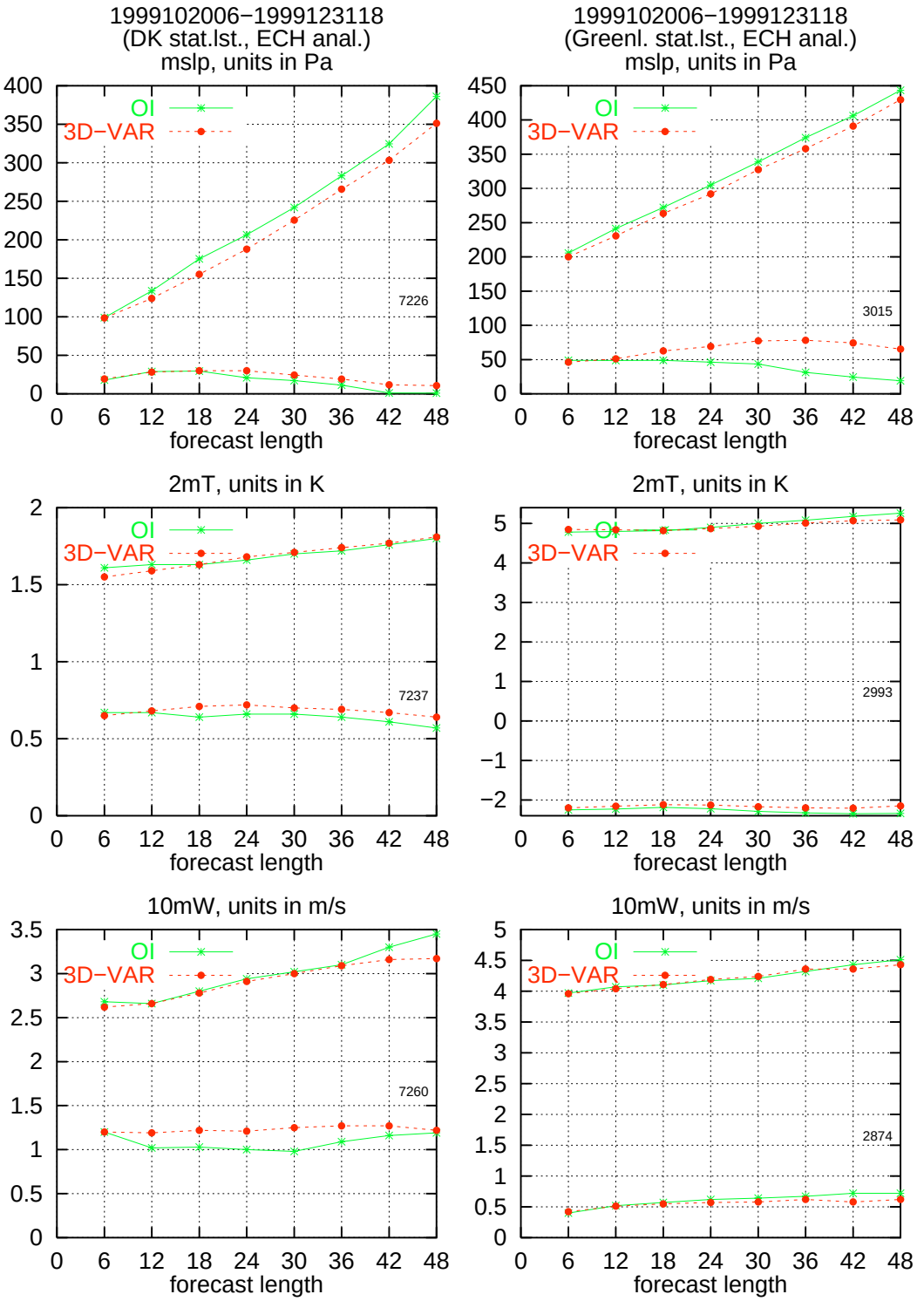

Figure 8: Observation verification scores (bias and RMS) for mean sea level pressure, 2 meter temperature and 10 meter wind, against Danish and Greenlandic stations for the period covering 1999102006 to 1999123118.

6.4 Field verification

In addition to the above described verification against observations we have also performed verification against analyses. Field verification can potentially give some information about the performance in areas with few observations such as over the oceans, but has the disadvantage that the quality of the verifying analyses in these data sparse areas is unknown. We verified the forecast against both the 3D-VAR analyses and the OI analyses. Due to a technical problem we had to split the period into two separate ones: one from 1999102006 to 1999113018, and another from 1999120100 to 1999123118. The verification scores of mean sea level pressure, 500 hPa geopotential height and 850 hPa temperature for these two sub-periods are given in table 1 and table 2, respectively.

		Against 3D-VAR Analyses				Against OI Analyses			
	Forecast	3D-VAR		OI		3D-VAR		OI	
Parameter	length	bias	RMS	bias	RMS	bias	RMS	bias	RMS
m.s.l.p.	12	0.11	1.26	0.07	1.92	0.14	1.71	0.10	1.56
(hPa)	24	0.16	1.92	0.11	2.62	0.19	2.19	0.13	2.34
	36	0.19	2.54	0.11	3.23	0.23	2.69	0.14	3.00
	48	0.20	3.14	0.10	3.75	0.24	3.21	0.14	3.56
500 hPa H	12	0.1	11.5	0.7	26.2	−1.3	24.1	−0.7	12.4
(gpm)	24	0.1	17.3	−0.1	30.1	−1.3	26.3	−1.5	18.5
	36	0.0	24.0	−0.9	34.9	−1.4	29.7	−2.3	25.2
	48	−0.1	30.8	−1.6	39.9	−1.5	33.8	−3.0	31.8
850 hPa T	12	−0.06	0.67	0.06	2.08	−0.25	2.26	−0.12	1.16
(K)	24	−0.11	1.10	−0.03	2.15	−0.30	2.37	−0.21	1.70
	36	−0.15	1.52	−0.10	2.32	−0.33	2.51	−0.27	2.13
	48	−0.17	1.92	−0.15	2.55	−0.35	2.65	−0.33	2.49

Table 1: Field verification scores for the period from 19991020 06Z to 19991130 18Z,

The results from the field verification are quite mixed. We have in principle four cases:

1. 3D-VAR based forecasts compared to 3D-VAR analyses and OI based forecasts compared to OI analyses: for this case the 3D-VAR runs have the lowest RMS and bias values for most parameters compared with the OI runs.

2. Both 3D-VAR and OI based forecasts are compared to 3D-VAR analyses: for this case the 3D-VAR results beats the OI ones on almost all RMS and bias values.

		Against 3D-VAR Analyses				Against OI Analyses			
	Forecast	3D-VAR		OI		3D-VAR		OI	
Parameter	length	bias	RMS	bias	RMS	bias	RMS	bias	RMS
m.s.l.p.	12	0.09	1.43	0.12	1.69	0.07	1.81	0.11	1.53
(hPa)	24	0.14	2.05	0.20	2.22	0.13	2.34	0.18	2.14
	36	0.16	2.61	0.23	2.72	0.14	2.84	0.21	2.68
	48	0.15	3.12	0.22	3.18	0.13	3.31	0.20	3.17
500 hPa H	12	−0.7	12.3	2.7	19.9	−4.8	19.9	−1.6	12.1
(gpm)	24	−1.0	17.7	1.7	24.0	−5.2	23.0	−2.5	17.1
	36	−1.7	23.1	0.7	27.1	−5.9	27.2	−3.6	22.4
	48	−2.7	28.8	−0.4	31.5	−6.7	31.9	−4.6	27.9
850 hPa T	12	−0.12	0.71	0.20	1.78	−0.50	2.13	−0.19	1.17
(K)	24	−0.19	1.16	0.05	1.80	−0.57	2.29	−0.34	1.64
	36	−0.25	1.58	−0.06	1.94	−0.63	2.48	−0.45	2.01
	48	−0.31	1.92	−0.15	2.12	−0.69	2.66	−0.43	2.30

Table 2: Same as in 1 but for the period from 19991201 00Z to 19991231 18Z.

3. 3D-VAR based forecasts compared to OI analyses and OI based forecasts compared to 3D-VAR analyses: For such a cross verification case OI beats 3D-VAR for most parameters.

4. Both 3D-VAR and OI based forecasts are compared to OI analyses: for this case OI beats 3D-VAR for all parameters except for mean sea level pressure in October/November 1999.

The above results reflects at best that the OI and 3D-VAR analyses are different, it can not be used to firmly state which analyses are better.

6.5 Results for the storm cases

We present here also some subjective verifications of the delayed mode 3D-VAR and OI runs for the four major storms in December 1999:

- The storm hitting Denmark on 3 December.
- The storm over Scotland on 25 December.
- The two storms over France on 26 and 27/28 December.

6.5.1 The Danish storm on 3 December

Figs. 9 and 10 show the 48, 36, 24, 18 and 12 hour forecasts and the analysis, all valid on 3 December 1999 at 18 Z from the 3D-VAR and the OI based delayed mode forecasts, respectively.

Comparing the results from the 3D-VAR run (Fig. 9) and OI run (Fig. 10), we see clearly that for this case the 3D-VAR runs perform significantly better than the corresponding OI runs. Both the position and depth of the low from the forecast based on 3D-VAR are significantly closer to the analyses than those based on OI analyses. However in these experiments we did not use the three hour data assimilation cycle and the merging procedure of ECMWF and HIRLAM analyses as in the operational suite. The difference between the two parallel runs might be smaller (and the results for both cases better) with a true operational "like" set-up.

6.5.2 The storms over Europe from the 25th to 28th of December

Figs. 11 and 12 show 48, 36, 24, 18 and 12 hour forecasts and analysis, all valid on 25 December 1999 00 Z from the 3D-VAR and the OI delayed mode runs, respectively, covering the storm passing Scotland that day. Figs. 13 and 14 show the corresponding model results valid on 26 December 1999 at 06 Z, covering the storm over France. At that time the low were centered near Le Havre. Finally in Figs. 15 and 16 we show the model results valid on 28 December 1999 00 Z, covering the second storm that affected France with the low centered near Dijon.

The overall results for the storms over Europe in this period are quite poor. Although the forecast by the 3D-VAR and OI runs are reasonably good for the storm over Scotland (Figs. 11 and 12), the two storms over France (Figs. 13 to 16) are poorly predicted. The last storm over France is slightly better predicted by the 3D-VAR runs compared to the OI runs, but neither are close in performance to those from the DMI operational runs, which predicted these storms quite well. The reason for this poor performance is under investigation, but preliminary results indicate that a 6 hour data assimilation cycle performs significantly worse than a corresponding 3 hour data assimilation cycle for these particular cases. The use of 6 hour data window may be blamed for failure in a few of these cases but more work needs to be done to verify this hypothesis.

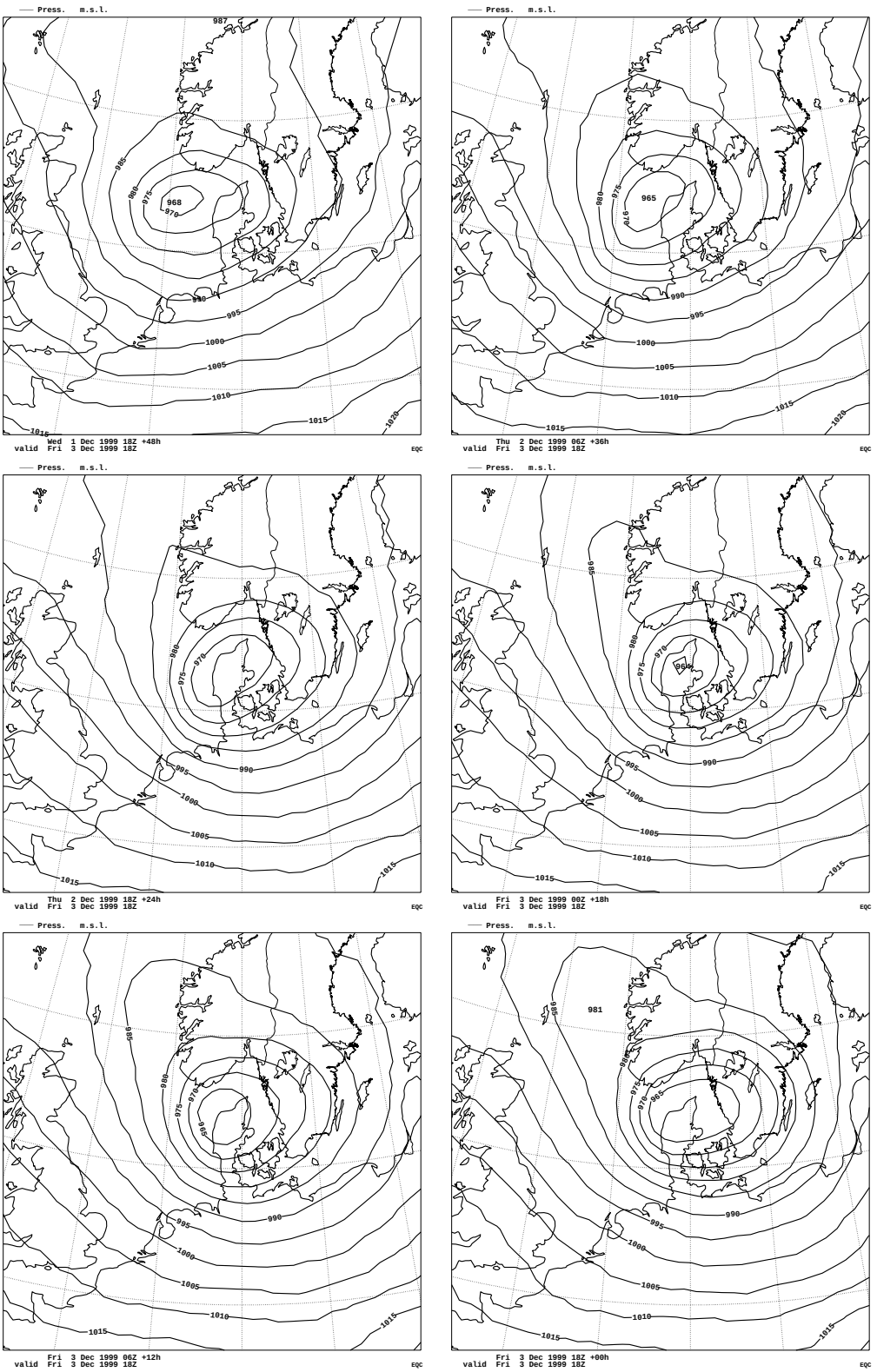

Figure 9: Forecasts (+48 hour, top left, +36 hour, top right, +24 hour, middle left, +18 hour, middle right and +12 hour, bottom left) and analysis (bottom right) valid at 19991203 18Z from the 3D-VAR delayed mode runs.

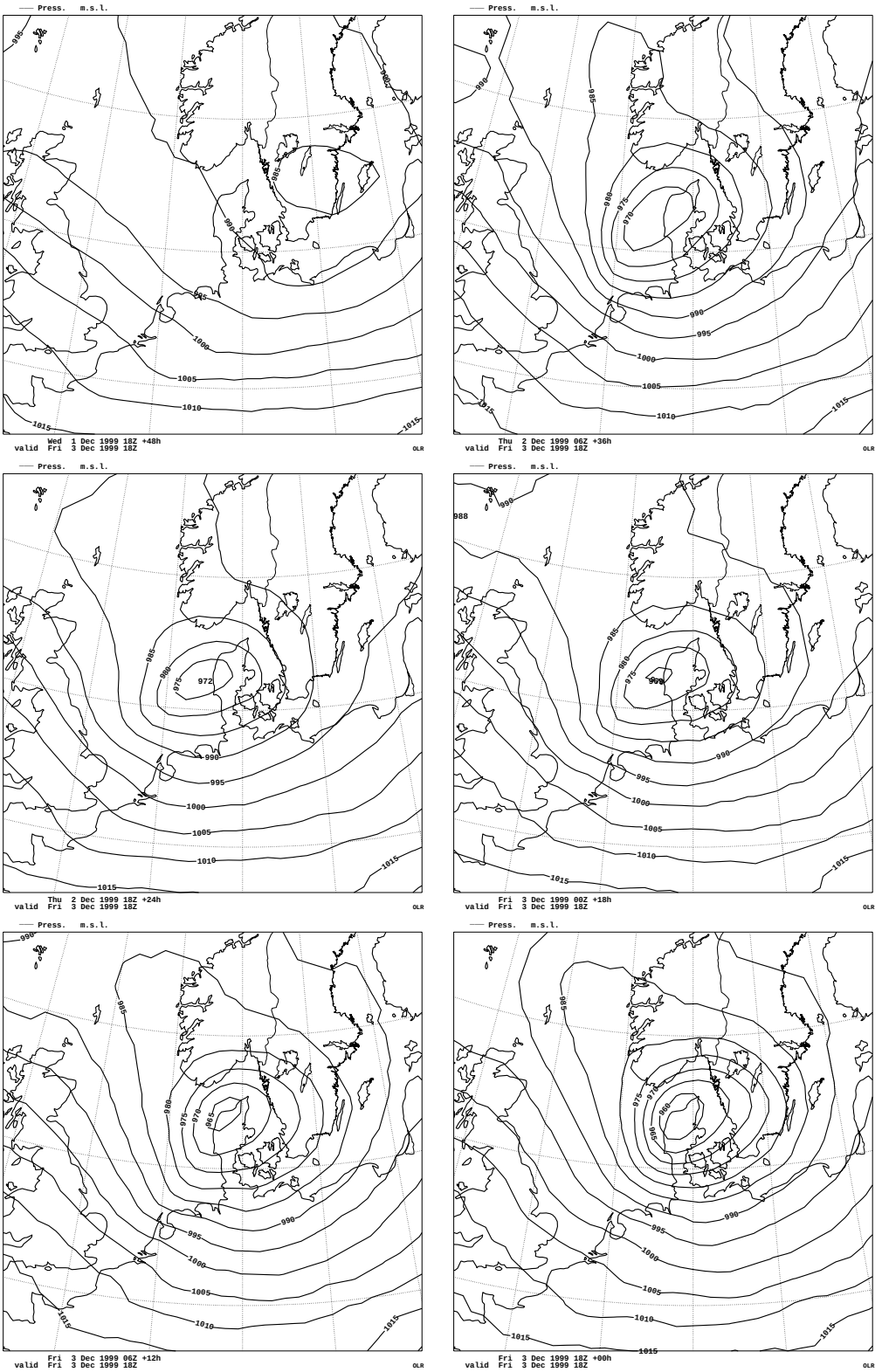

Figure 10: As Fig. 9 but from the OI delayed mode runs.

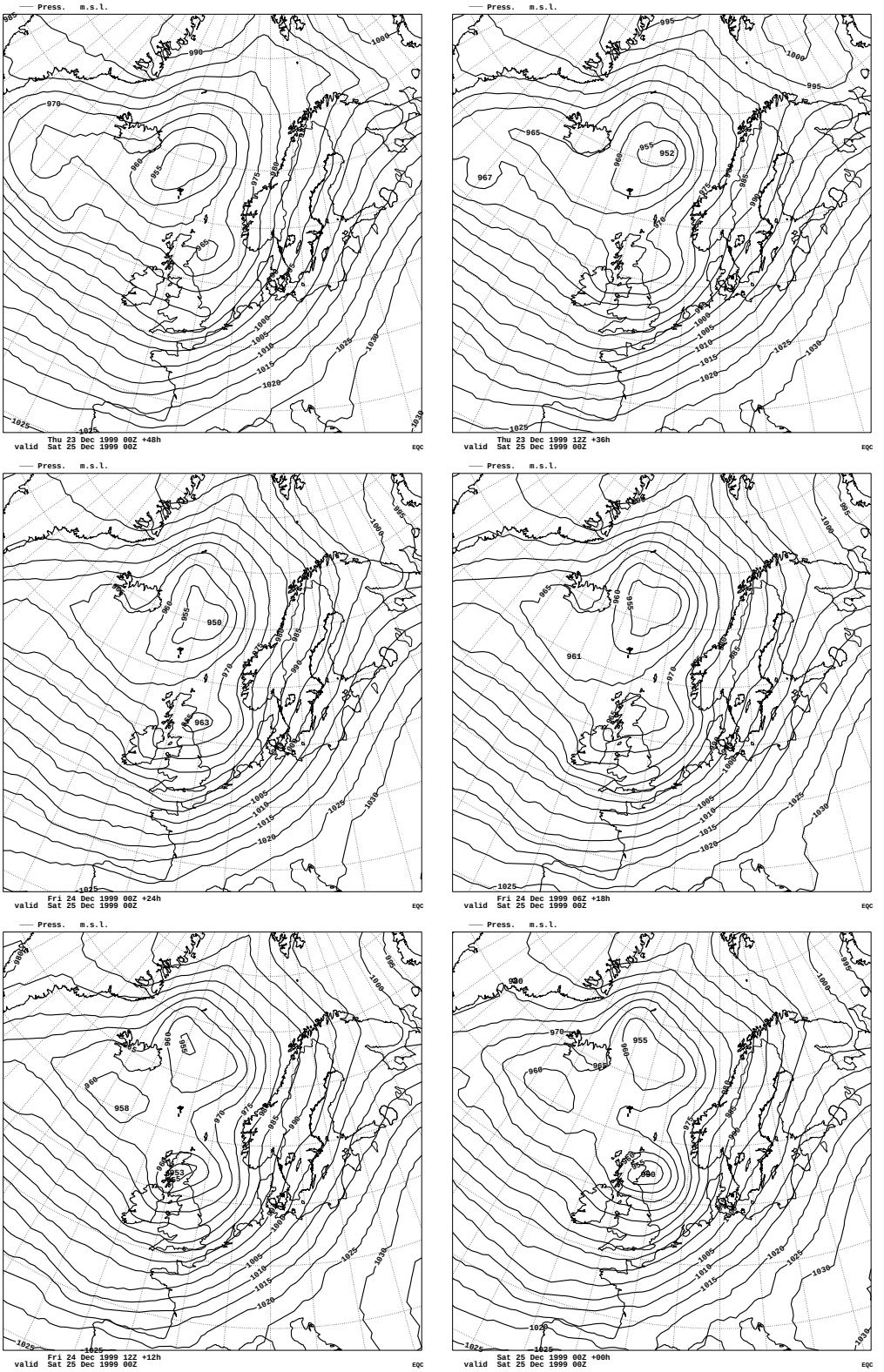

Figure 11: As Fig. 9 but valid at 19991225 00Z from the 3D-VAR delayed mode runs.

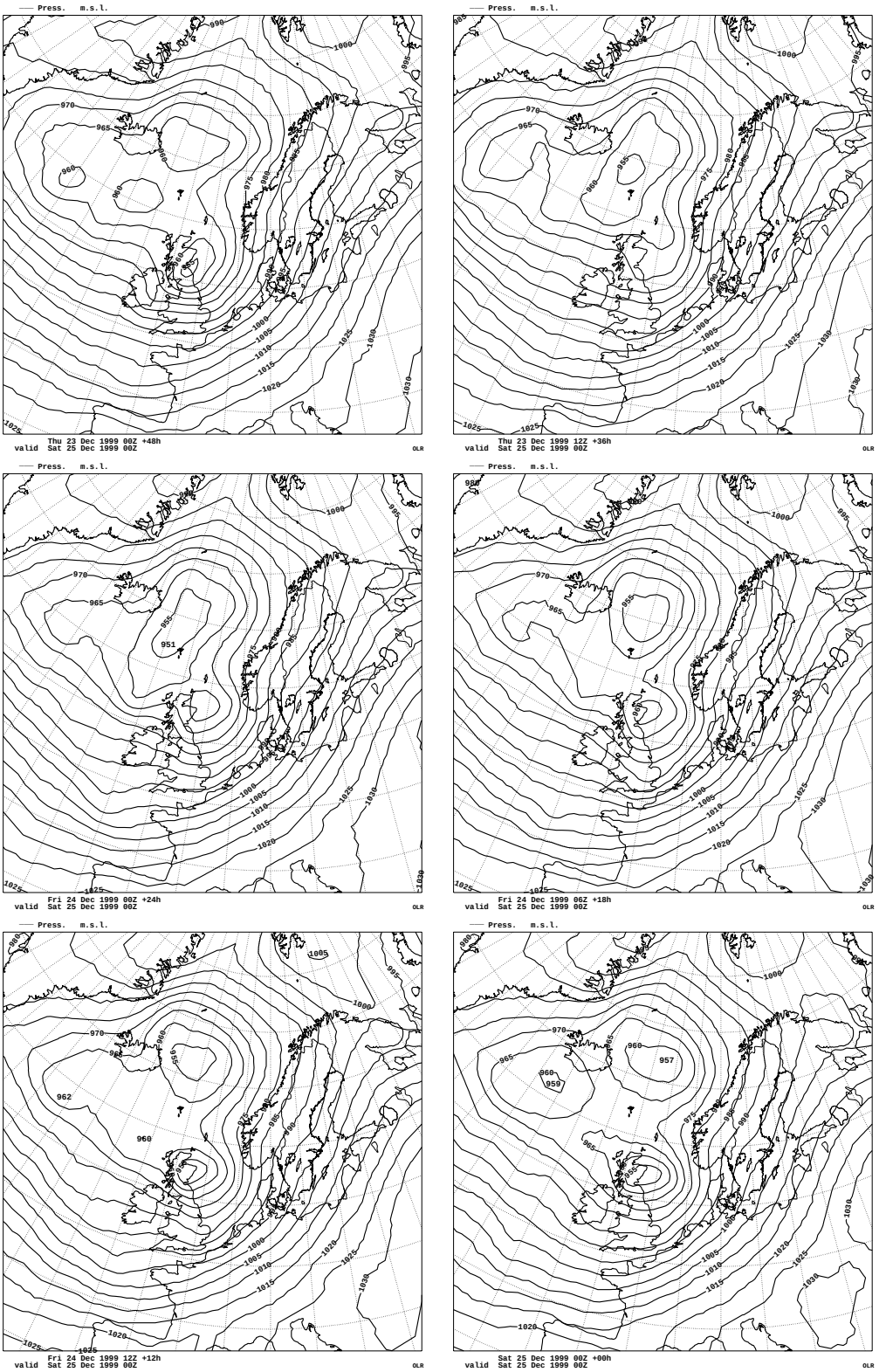

Figure 12: As Fig. 11 but from the OI delayed mode runs.

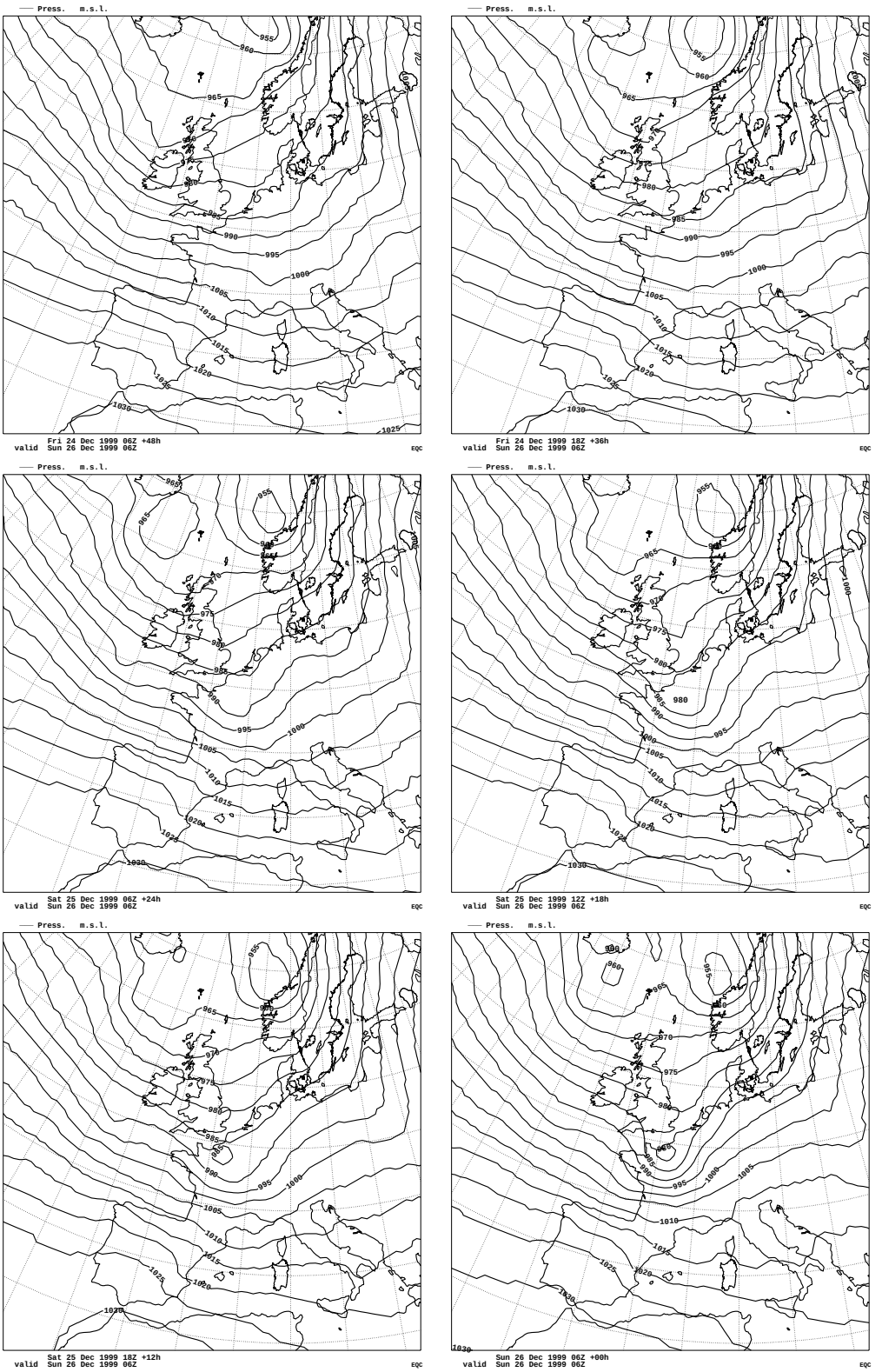

Figure 13: As Fig. 9 but valid at 19991226 06Z from the 3D-VAR delayed mode runs.

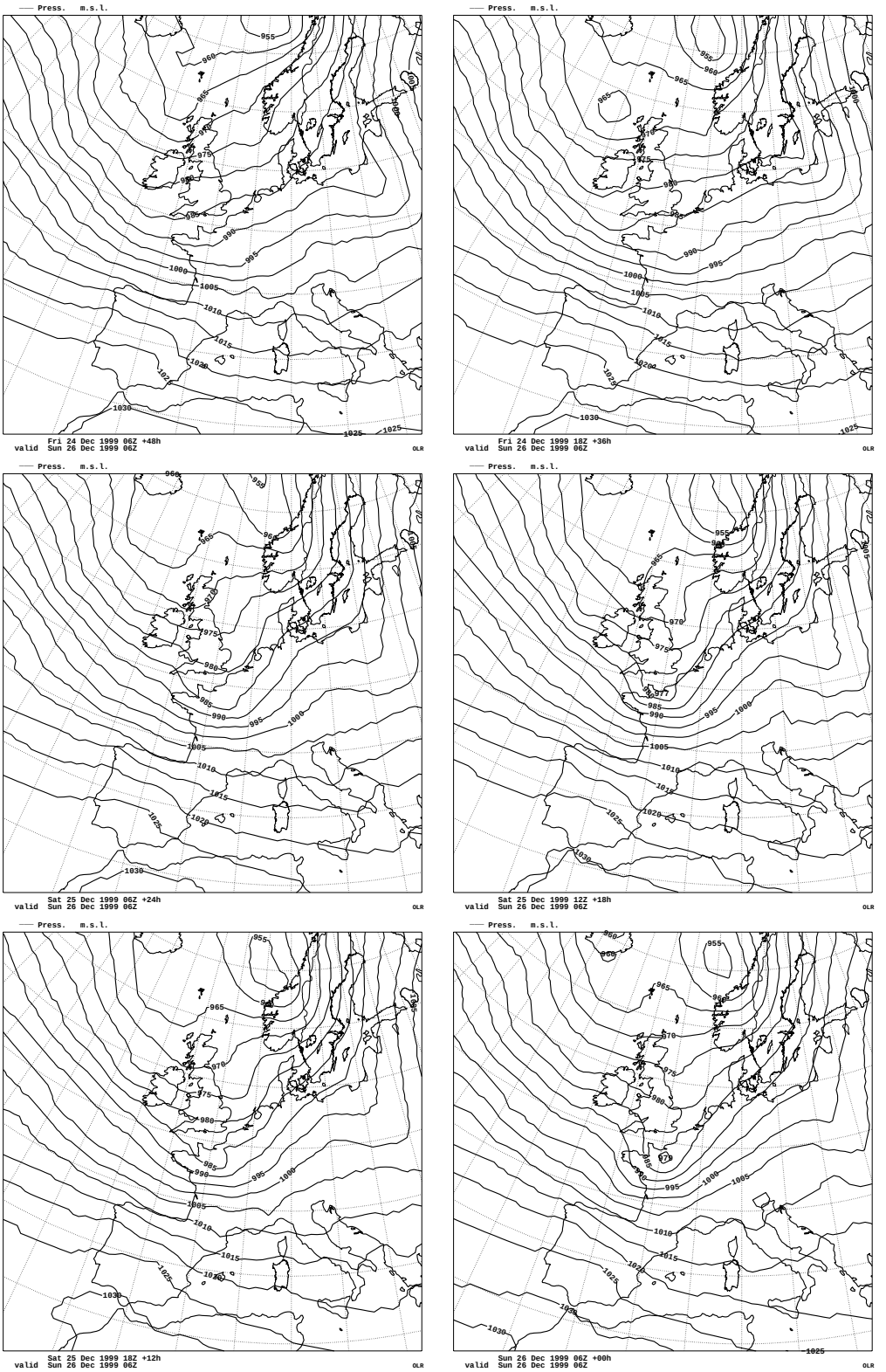

Figure 14: As Fig. 13 from the OI delayed mode runs.

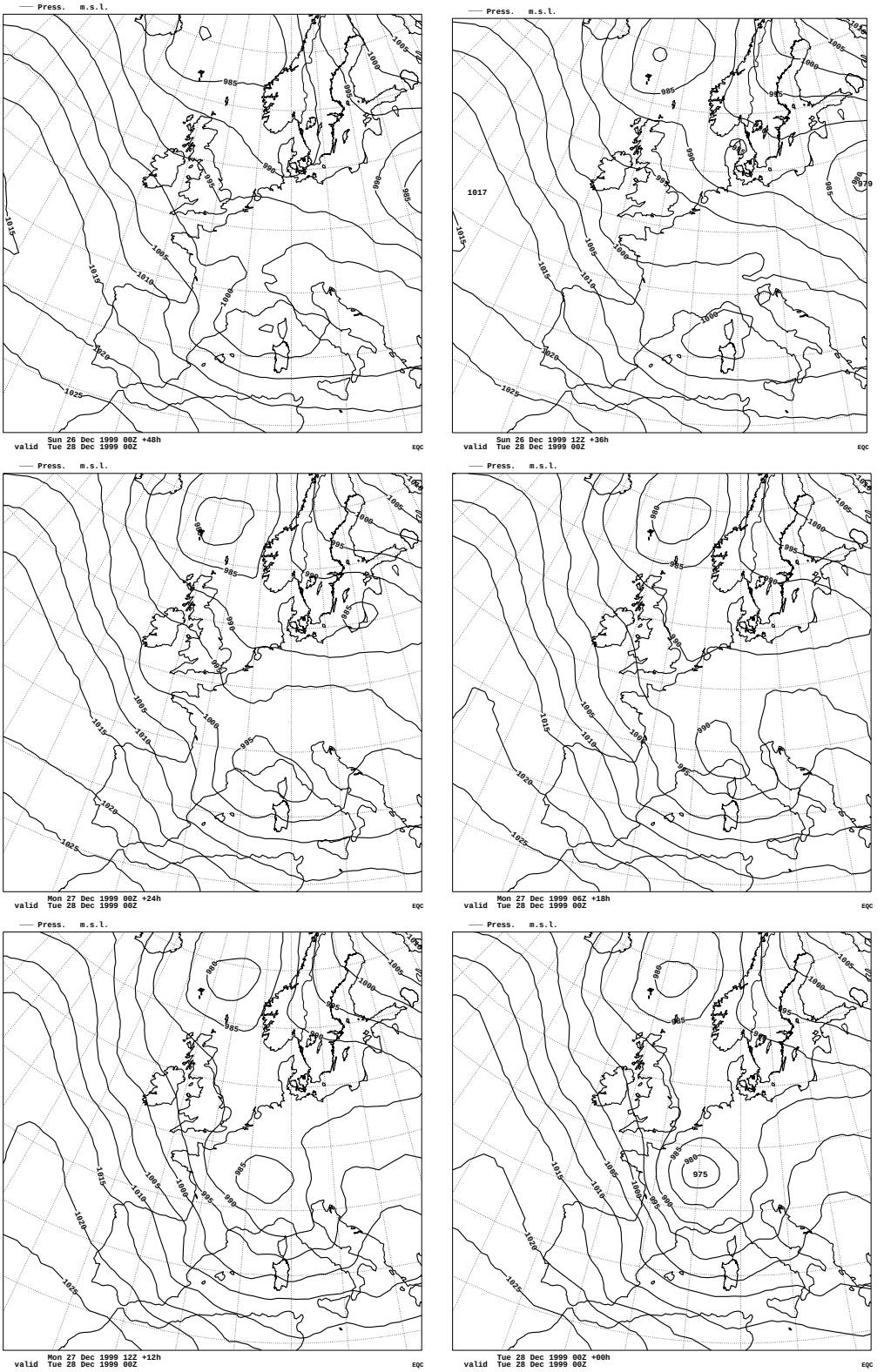

Figure 15: As Fig. 9 but valid at 19991228 00Z from the 3D-VAR delayed mode runs.

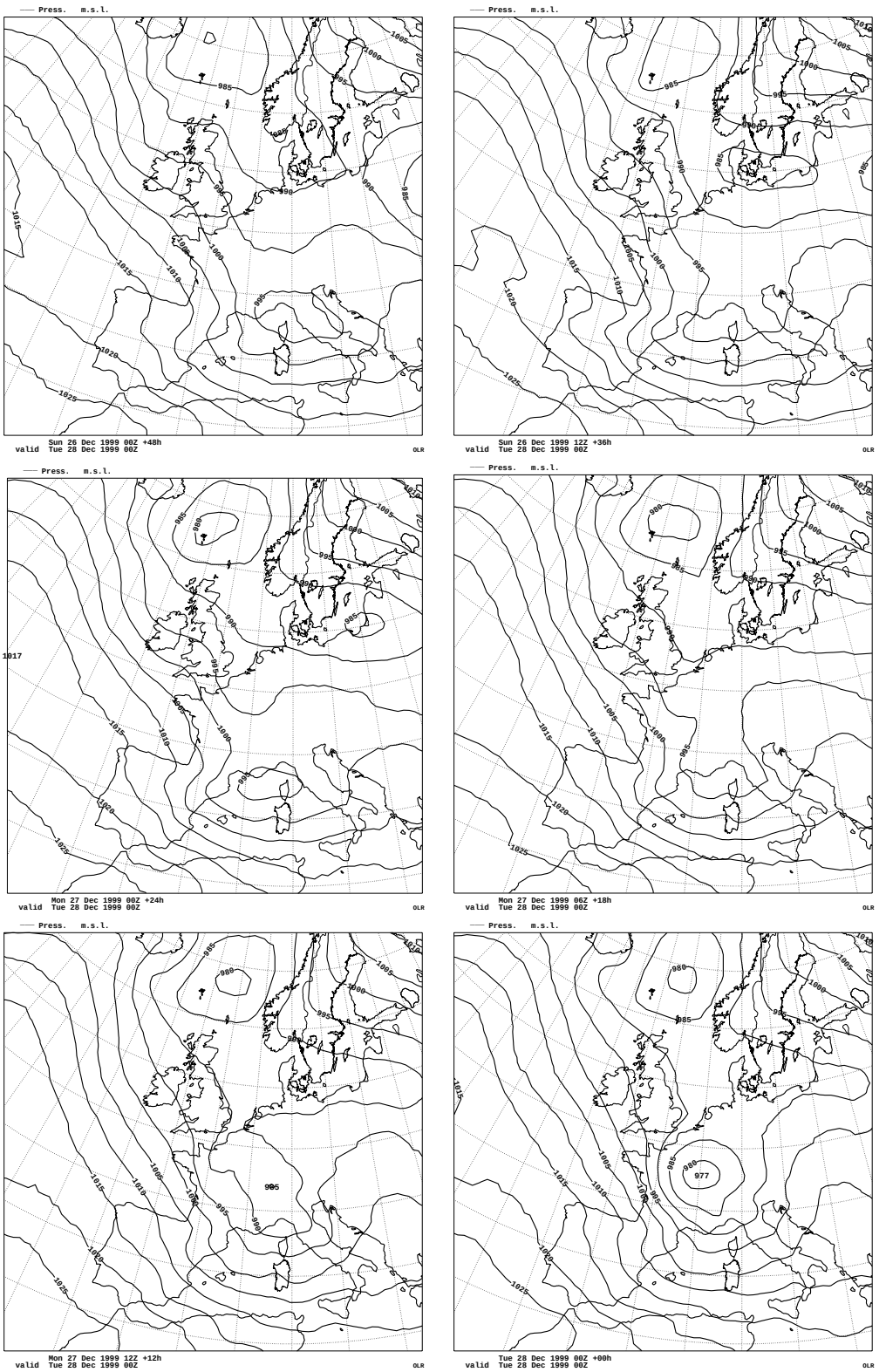

Figure 16: As Fig. 15 but from the OI delayed mode runs.

7 Results of pre-operational runs

We will now discuss the results of pre-operational runs based on observation verification. The discussion will not be as detailed as for the delayed-mode runs, since many of the conclusions are similar.

7.1 Observation verification against EWGLAM stations

Figs. 17 to 19 and Figs. 20 to 22 show the verification against observations from the EWGLAM station list for the pre-operational parallel runs for June and July 2000 respectively. The verification set-up is similar to the above described one for the delayed-mode runs.

The most fair comparison between OI and 3D-VAR based forecasts is to compare the six hour data assimilation runs (experiment ASG using OI and experiment ASE using 3D-VAR). During the first 14 days of June 2000 these two experiments used climatic sea surface temperatures instead of updated ECMWF sea surface temperatures (as in the operational set-up) due to an error. The consequence of this error is reflected in the significant negative biases for the 2 meter and 850 hPa temperature in June 2000 for both experiments (Figs. 17 and 18).

Overall almost identical conclusions can be made about the observation verification of the pre-operational runs as for the delayed mode runs. The 3D-VAR runs (ASE) has better or similar RMS scores for all parameters compared to the OI runs (ASG) for both months. As in the delayed-mode runs, the results are consistently slightly better for the 3D-VAR runs compared with the corresponding OI runs. Again, the main significant improvement is seen in 250 hPa level, where the fact that the 3D-VAR analysis scheme use radio soundings from all significant levels seems to give a clear improvement in RMS score for temperature.

Comparing with the operational OI runs (G45 in the Figs.) we see that both the pre-operational 3D-VAR (ASE) and OI (ASG) seems to do better or similar to the operational system. The comparision is not clean since also forecast code is different, so caution should be taken when comparing the pre-operational runs with the operational runs.

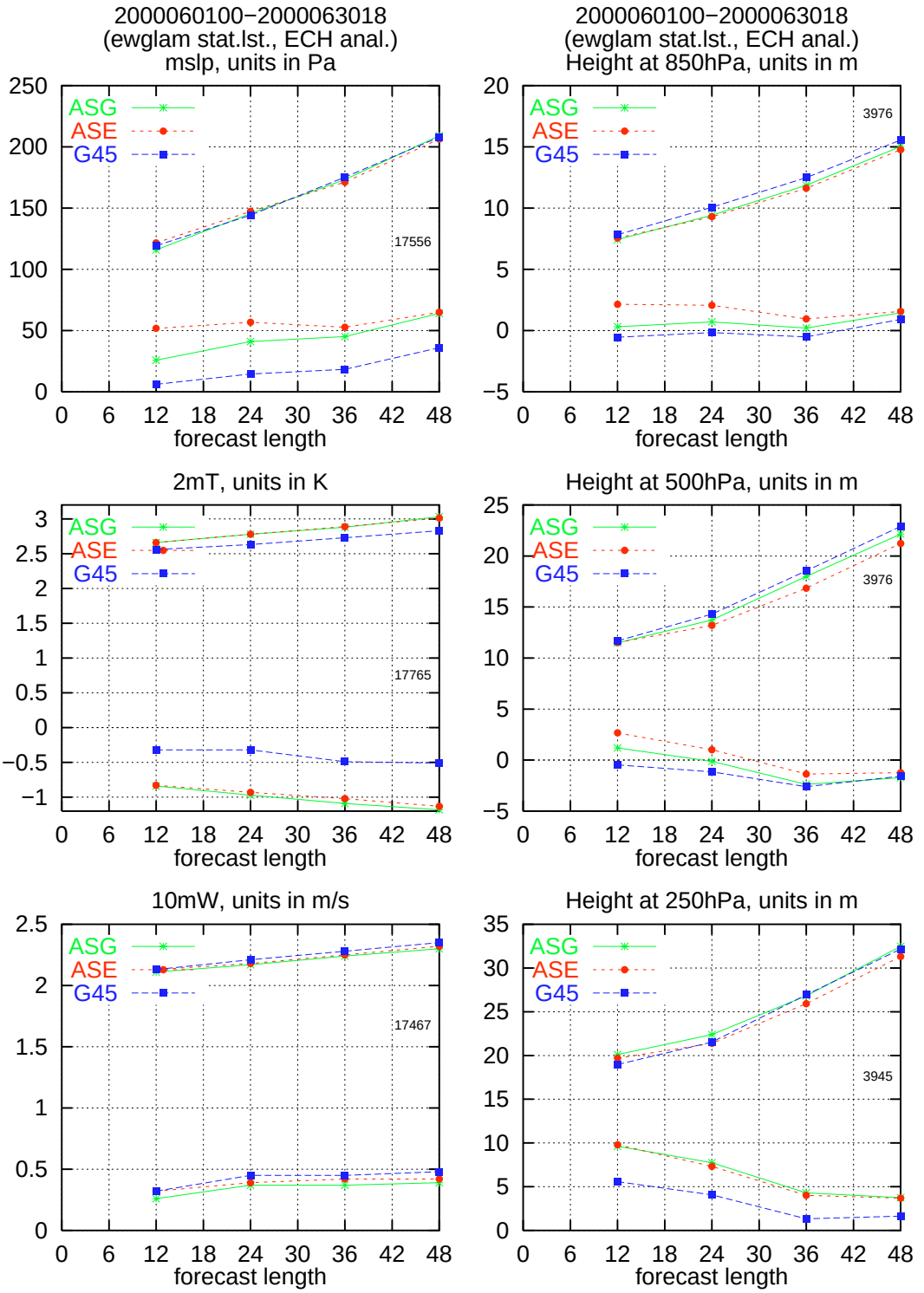

Figure 17: Observation verification scores (bias and RMS) against EWGLAM stations of the pre-operational runs for June 2000 for mean sea level pressure, 2 meter temperature, 10 meter wind, and height at 850 hPa, 500 hPa, and 250 hPa. In the figure the experiment names correspond to the following: G45 refers the operational HIRLAM-G runs (3-hour data assimilation cycle), ASE the 3D-VAR HIRLAM-G runs (6-hour data assimilation cycle) and ASG the OI HIRLAM-G runs (6-hour data assimilation cycle).

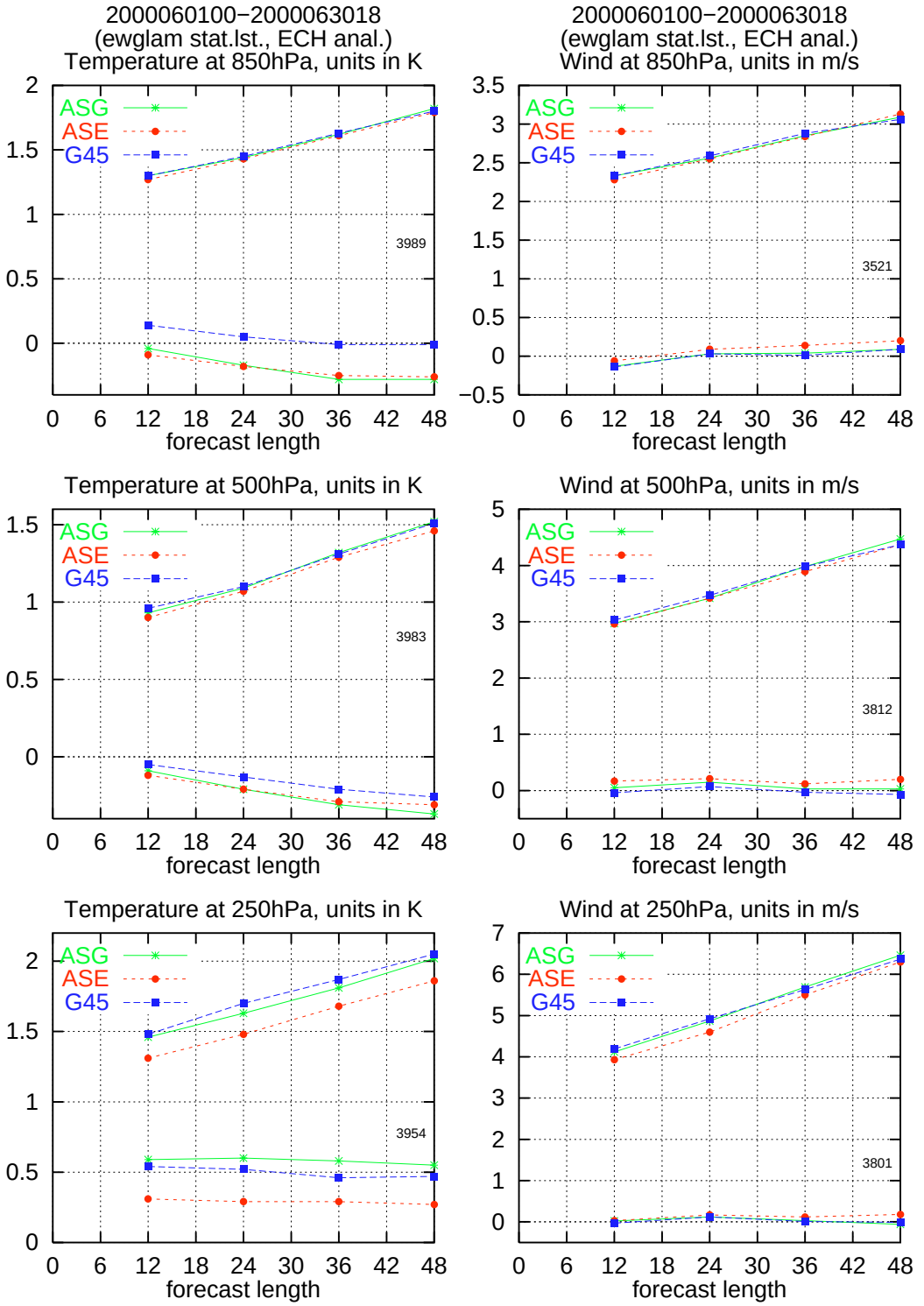

Figure 18: Same as in Fig. 17 but for temperature and wind at 850 hPa, 500 hPa, and 250 hPa.

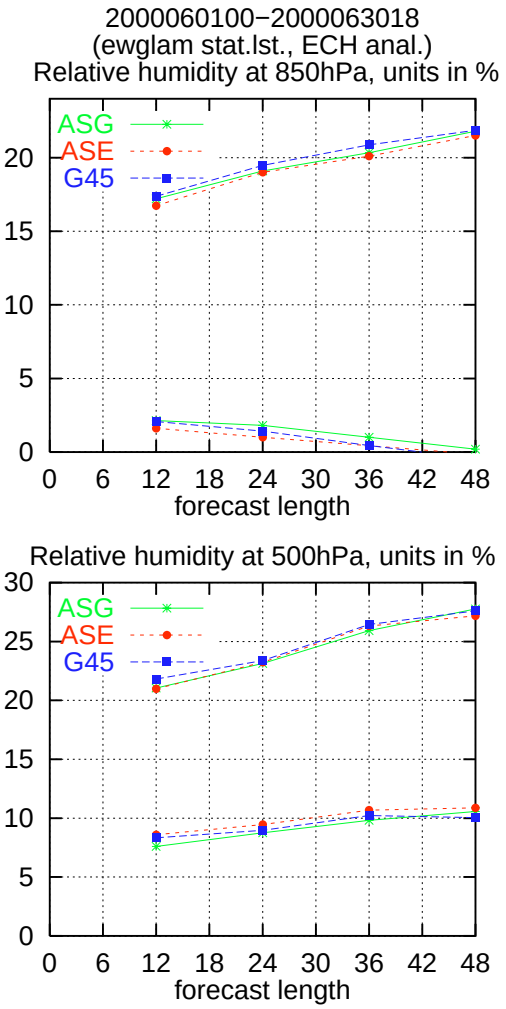

Figure 19: Same as in Fig. 17 but for relative humidity at 850 hPa and 500 hPa.

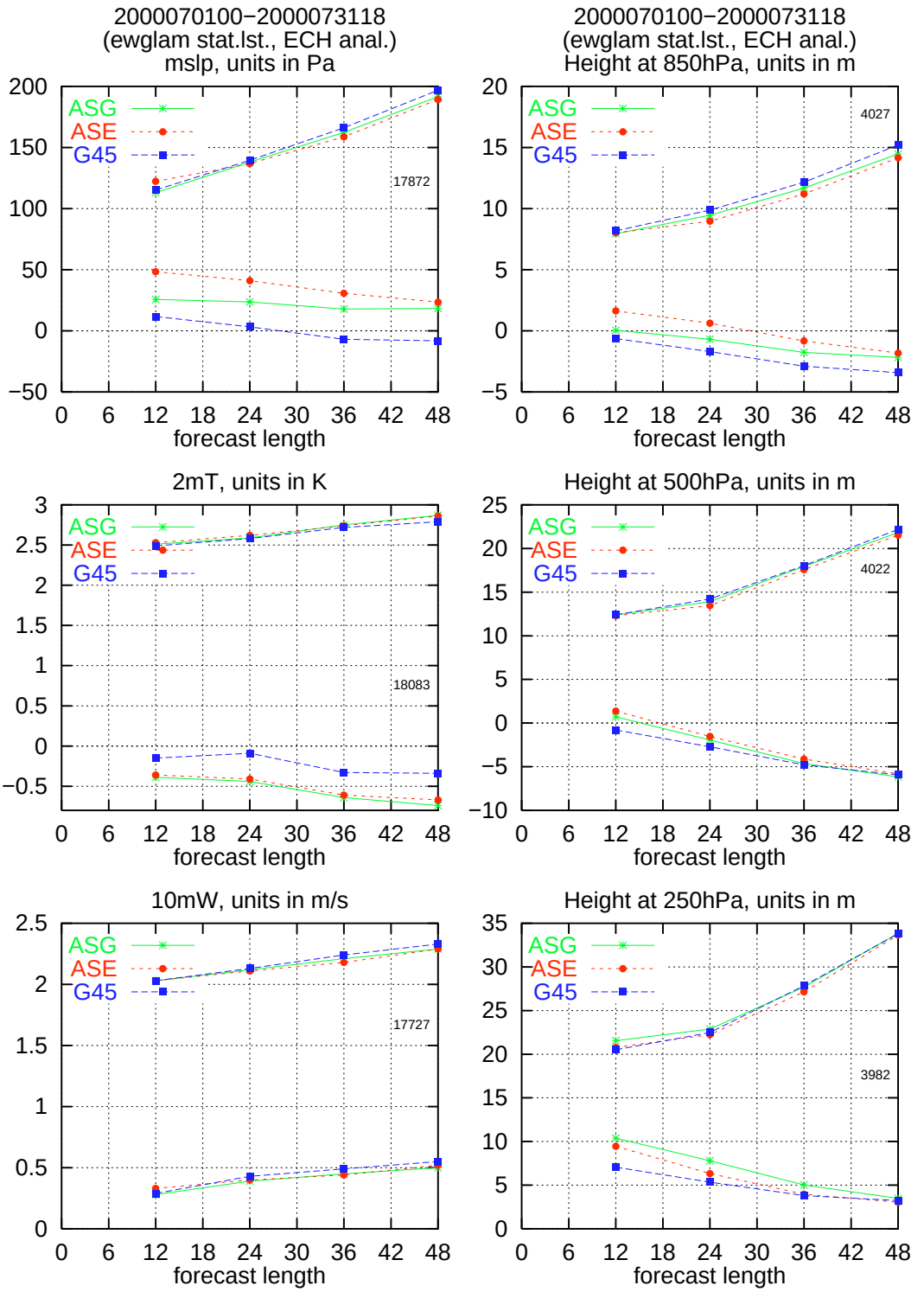

Figure 20: Same as in Fig. 17 but for July 2000.

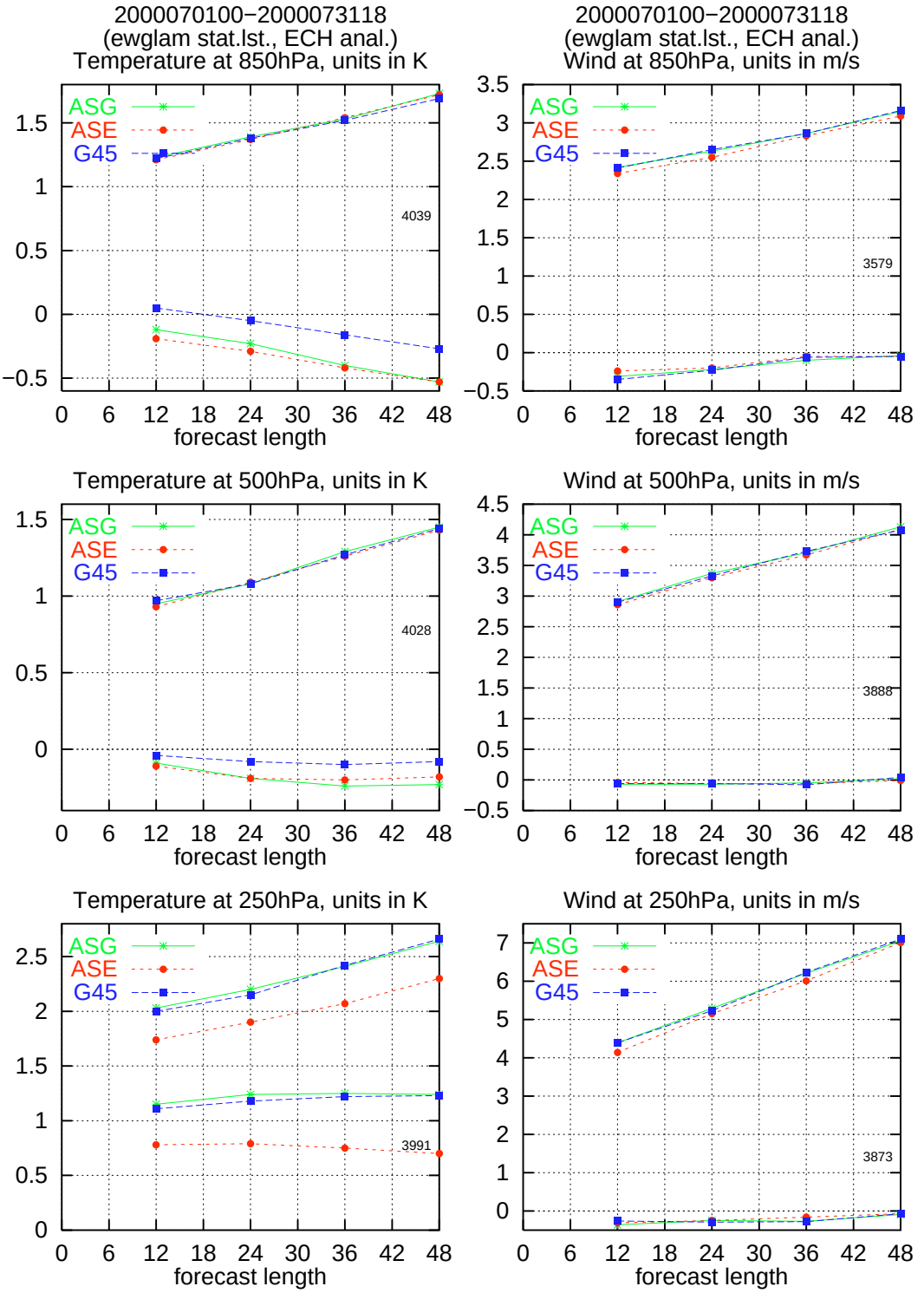

Figure 21: Same as in Fig. 20 but for temperature and wind at 850 hPa, 500 hPa and 250 hPa.

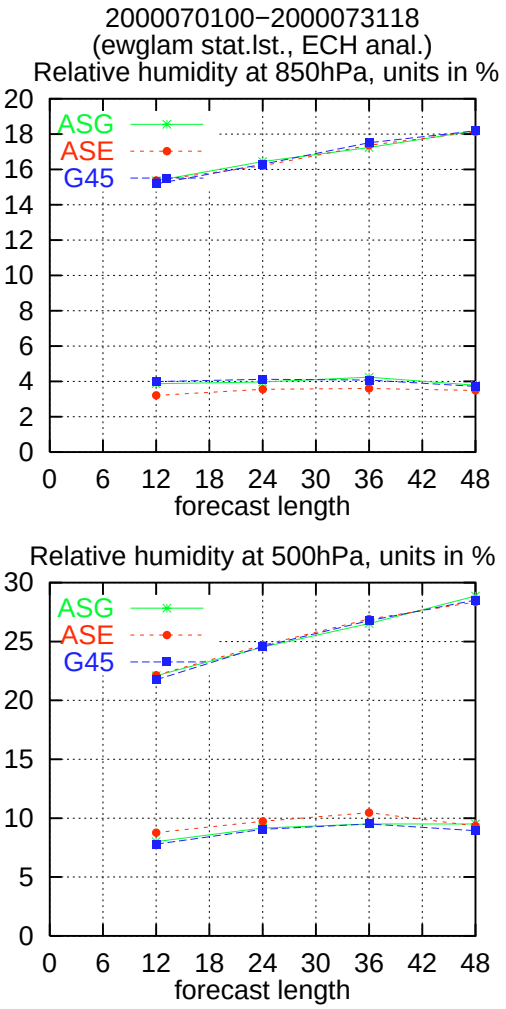

Figure 22: Same as in Fig. 20 but for relative humidity at 850 hPa and 500 hPa.

7.2 Precipitation verification

We have also looked at the precipitation verification against Danish SYNOP stations in form of contingency tables where 12 hour precipitation is divided into 5 classes of precipitation and the number of hits are counted. The 5 precipitation classes are (precipitation amounts in mm): $P1 < 0.2$, $0.2 \leq P2 < 1.0$, $1.0 \leq P3 < 5$, $5 \leq P4 < 10$ and $P4 \geq 10$ with P being either F (forecast) or O (observation).

The results are shown for June and July 2000 in Table 3. With a perfect forecast all non-zero numbers would be in the diagonal.

The tables show that the 3D-VAR runs seem to produce slightly more forecasts which fall into the correct class (larger numbers in the diagonal) compared to the OI runs. However, in both 3D-VAR and OI runs there were a few bad cases where the forecasts predict class F5 but observations fall into O1 and vice versa. In general the forecasts seems to over-predict the amount of precipitation compared to the observed values. This is a known problem of the HIRLAM model.

G45 0006							G45 0007						
	O1	O2	O3	O4	O5	sum		O1	O2	O3	O4	O5	sum
F1	**520**	13	9	0	0	542	F1	**504**	25	10	2	**3**	544
F2	294	**46**	38	9	1	388	F2	351	**47**	19	13	3	433
F3	43	45	**76**	20	15	199	F3	53	22	**36**	10	4	125
F4	4	7	21	**15**	3	50	F4	0	0	2	**9**	0	11
F5	**1**	2	9	4	**4**	19	F5	0	0	1	8	**7**	16
sum	862	113	153	48	22	1198	sum	908	94	68	42	17	1129
%FO	60	41	50	31	14	55	%FO	56	50	53	21	41	53

ASE 0006							ASE 0007						
	O1	O2	O3	O4	O5	sum		O1	O2	O3	O4	O5	sum
F1	**524**	13	7	2	**1**	547	F1	**529**	22	13	8	**3**	575
F2	262	**48**	30	5	3	248	F2	339	**49**	24	6	3	421
F3	54	47	**81**	18	12	212	F3	38	22	**27**	10	4	101
F4	1	3	25	**16**	3	48	F4	1	0	4	**15**	5	25
F5	**1**	2	10	7	**3**	23	F5	**1**	1	0	3	**2**	7
sum	842	113	153	48	22	1178	sum	908	94	68	42	17	1129
%FO	62	42	53	33	14	57	%FO	58	52	40	36	12	55

ASG 0006							ASG 0007						
	O1	O2	O3	O4	O5	sum		O1	O2	O3	O4	O5	sum
F1	**507**	10	8	0	0	525	F1	**483**	24	10	4	**2**	523
F2	283	**47**	34	4	2	370	F2	355	**46**	19	6	7	433
F3	47	46	**72**	18	14	197	F3	67	24	**33**	14	1	139
F4	4	8	29	**14**	3	58	F4	3	0	4	**7**	1	15
F5	**1**	2	10	12	**3**	28	F5	0	0	2	11	**6**	19
sum	842	113	153	48	22	1178	sum	908	94	68	42	17	1129
%FO	60	42	47	29	17	55	%FO	53	49	49	17	35	51

Table 3: Contingency tables of 12 hour accumulated precipitation (6 hours to 18 hour forecast interval) for the pre-operational runs in June (left) and July (right) 2000. The %FO number is number (in percent) of correct forecasts for a given observed precipition class. G45 denotes the operational HIRLAM-G runs (3-hour data assimilation cycle), ASE the 3D-VAR HIRLAM-G runs (6-hour data assimilation cycle) and ASG the OI HIRLAM-G runs (6-hour data assimilation cycle).

8 Conclusions

In this report we have shown that the current version of the HIRLAM 3D-VAR system can produce analyses which give forecast as least as good as those produced by the HIRLAM OI system both in delayed mode and in pre-operational mode (with real-time input data). The improvement of the 3D-VAR runs over the OI runs are small but consistent, which is sufficient to justify an operational implementation due to the many potentials of the 3D-VAR system in improving data assimilation, notably in the use of new types of observation data, which has been difficult or impossible within an OI framework.

Ensuring the stability of the code is the second important issue before an operational implementation of HIRLAM 3D-VAR at DMI. As mentioned above the last upgrade of 3D-VAR pre-operational set-up was done in mid-May 2000. Since then there has been no problem with stability, so it seems that the code is sufficiently stable for an operational implementation.

A HIRLAM 3D-VAR analysis takes significantly longer computer time compared to a HIRLAM OI analysis. Our experiences however suggest that the time required for a 3D-VAR analysis is within limits which allow operational deadlines to be met. However, we may need to improve the efficiency of the programs in order to save time which become necessary when more observations and higher resolution models with more grid-points are introduced.

With the fulfillment of the three main criteria for an operational implementation, *i.e.* good results, stable code and sufficient short execution time, we see no major problem with making the HIRLAM 3D-VAR system operational for the DMI-HIRLAM-G area.

Currently we are in the process of investigating the effect of going to a 3-hour data assimilation cycle instead of the 6-hour data assimilation cycle used in the described experiments.

In the future we will focus our operational oriented 3D-VAR development work on investigating the effects of going to higher resolutions in order to run 3D-VAR on the operational high resolution areas. We will also start to work on the use of satellite data and other new observation types in the 3D-VAR framework.

Based on the results presented in this report and additional parallel runs with OI and 3D-VAR (not shown) we made the HIRLAM 3D-VAR system part of the operational upgrade on 26 September 2000 for the HIRLAM-G model. We still use the HIRLAM OI system on the high resolution model versions.

References

Andersson, E., and Järvinen, H. 1999. Variational Quality Control. *Q. J. R. Meteorol. Soc.*, **125**, 697–722.

Berre, Loik. 1997. *Non-separable Structure Functions for HIRLAM 3D-VAR.* Technical Report 30. Hirlam 4 project, c/o Met Éireann, Glasnevin Hill, Dublin 9, Ireland.

Dragosavac, M. 1994. *BUFR User guide and reference manual.* European Centre for Medium-Range Weather Forecasts.

ECMWF. 1999. *Integrated forecasting system, Technical documentation, Part I, Observation processing.* European Centre for Medium-Range Weather Forecasts. Internal document within HIRLAM and ECMWF.

Gilbert, J. C., and Lemaréchal, C. 1989. Some numerical experiments with variable storage quasi-Newton algorithms. *Math. Prog.*, **B24**, 407–435.

Gustafsson, N., Hörnquist, S., Lindskog, M., Berre, L., Navascués, B., Thorsteinsson, Sigurdur, Huang, Xiang-Yu, Mogensen, Kristian S., and Rantakokko, Jarmo. 1999. *Three-dimensional variational data assimilation for a high resolution limited area model (HIRLAM).* Technical Report 40. Hirlam 4 project, c/o Met Éireann, Glasnevin Hill, Dublin 9, Ireland.

Gustafsson, N., Berre, L., Hörnquist, S., Huang, X.-Y., Lindskog, M., Navascués, B., Mogensen, K. S., and Thorsteinsson, S. 2000. Three-dimensional variational data assimilation for a limited area model. Part I: General formulation and the background error constraint. *Accepted by Tellus.*

Hollingsworth, A., and Lönnberg, P. 1986. The statistical structure of short-range forecast errors as determined from radiosonde data. Part I: The wind field. *Tellus*, **38A**, 111–136.

Lindskog, M., and Gustafsson, N. 1998. A parallel 3-Diminsional variational data assimilation system for Hirlam. *In:* Hoffmann, Geerd-R, and Kreitz, Norbert (eds), *Proceedings of the Eight ECMWF Workshop on the Use of Parallel Processors in Meteorology.* World Scientific.

Lindskog, M., Gustafsson, N., Navascués, B., Mogensen, K. S., Huang, X.-Y., Yang, X., Andræ, U., Berre, L., Thorsteinsson, S., and Rantakko, J. 2000. Three-dimensional variational data assimilation for a limited area model. Part II: Observation handling and assimilation experiments. *Accepted by Tellus.*

Lönnberg, P., and Hollingsworth, A. 1986. The statistical structure of short-range forecast errors as determined from radiosonde data. Part II: The covariance of height and wind errors. *Tellus*, **38A**(137-161).

Lorenc, A. C. 1986. Analysis methods for numerical weather prediction. *Q. J. Roy. Met. Soc.*, **113**, 1177–1194.

Saarinen, Sami. 2000. Private communications.

Sass, Bent Hansen, Nielsen, Niels Woetmann, Jørgensen, Jess U., and Amstrup, Bjarne. 1999. *The operational HIRLAM system at DMI - October 1999* -. Technical Report 99-21. Danish Meteorological Institute.

WMO. 1995. *Manual on codes, Volume I, International codes, Part B - Binary codes.* No 306, fm-94-ix, ext. bufr edn.

DANISH METEOROLOGICAL INSTITUTE

Scientific Reports

Scientific reports from the Danish Meteorological Institute cover a variety of geophysical fields, i.e. meteorology (including climatology), oceanography, subjects on air and sea pollution, geomagnetism, solar-terrestrial physics, and physics of the middle and upper atmosphere.

Reports in the series within the last five years:

No. 95-1
Peter Stauning and T.J. Rosenberg:
High-Latitude, day-time absorption spike events
1. morphology and occurrence statistics
Not published

No. 95-2
Niels Larsen: Modelling of changes in stratospheric ozone and other trace gases due to the emission changes : CEC Environment Program Contract No. EV5V-CT92-0079. Contribution to the final report

No. 95-3
Niels Larsen, Bjørn Knudsen, Paul Eriksen, Ib Steen Mikkelsen, Signe Bech Andersen and Torben Stockflet Jørgensen: Investigations of ozone, aerosols, and clouds in the arctic stratosphere : CEC Environment Program Contract No. EV5V-CT92-0074. Contribution to the final report

No. 95-4
Per Høeg and Stig Syndergaard: Study of the derivation of atmospheric properties using radio-occultation technique

No. 95-5
Xiao-Ding Yu, **Xiang-Yu Huang** and **Leif Laursen** and Erik Rasmussen: Application of the HIRLAM system in China: heavy rain forecast experiments in Yangtze River Region

No. 95-6
Bent Hansen Sass: A numerical forecasting system for the prediction of slippery roads

No. 95-7
Per Høeg: Proceeding of URSI International Conference, Working Group AFG1 Copenhagen, June 1995. Atmospheric research and applications using observations based on the GPS/GLONASS System
Not published

No. 95-8
Julie D. Pietrzak: A comparison of advection schemes for ocean modelling

No. 96-1
Poul Frich (co-ordinator), H. Alexandersson, J. Ashcroft, B. Dahlström, G.R. Demarée, A. Drebs, A.F.V. van Engelen, E.J. Førland, I. Hanssen-Bauer, R. Heino, T. Jónsson, K. Jonasson, L. Keegan, P.Ø. Nordli, **T. Schmith**, **P. Steffensen**, H. Tuomenvirta, O.E. Tveito: North Atlantic Climatological Dataset (NACD Version 1) - Final report

No. 96-2
Georg Kjærgaard Andreasen: Daily response of high-latitude current systems to solar wind variations: application of robust multiple regression. Methods on Godhavn magnetometer data

No. 96-3
Jacob Woge Nielsen, Karsten Bolding Kristensen, Lonny Hansen: Extreme sea level highs: a statistical tide gauge data study

No. 96-4
Jens Hesselbjerg Christensen, Ole Bøssing Christensen, Philippe Lopez, Erik van Meijgaard, Michael Botzet: The HIRLAM4 Regional Atmospheric Climate Model

No. 96-5
Xiang-Yu Huang: Horizontal diffusion and filtering in a mesoscale numerical weather prediction model

No. 96-6
Henrik Svensmark and Eigil Friis-Christensen: Variation of cosmic ray flux and global cloud coverage - a missing link in solar-climate relationships

No. 96-7
Jens Havskov Sørensen and Christian Ødum Jensen: A computer system for the management of epidemiological data and prediction of risk and economic consequences during outbreaks of foot-and-mouth disease. CEC AIR Programme. Contract No. AIR3 - CT92-0652

No. 96-8
Jens Havskov Sørensen: Quasi-automatic of input for LINCOM and RIMPUFF, and output conversi-

on. CEC AIR Programme. Contract No. AIR3 - CT92-0652

No. 96-9
Rashpal S. Gill and Hans H. Valeur:
Evaluation of the radarsat imagery for the operational mapping of sea ice around Greenland

No. 96-10
Jens Hesselbjerg Christensen, Bennert Machenhauer, Richard G. Jones, Christoph Schär, Paolo Michele Ruti, Manuel Castro and Guido Visconti:
Validation of present-day regional climate simulations over Europe: LAM simulations with observed boundary conditions

No. 96-11
Niels Larsen, Bjørn Knudsen, Paul Eriksen, Ib Steen Mikkelsen, Signe Bech Andersen and Torben Stockflet Jørgensen: European Stratospheric Monitoring Stations in the Artic: An European contribution to the Network for Detection of Stratospheric Change (NDSC): CEC Environment Programme Contract EV5V-CT93-0333: DMI contribution to the final report

No. 96-12
Niels Larsen: Effects of heterogeneous chemistry on the composition of the stratosphere: CEC Environment Programme Contract EV5V-CT93-0349: DMI contribution to the final report

No. 97-1
E. Friis Christensen og C. Skøtt: Contributions from the International Science Team. The Ørsted Mission - a pre-launch compendium

No. 97-2
Alix Rasmussen, Sissi Kiilsholm, Jens Havskov Sørensen, Ib Steen Mikkelsen: Analysis of tropospheric ozone measurements in Greenland: Contract No. EV5V-CT93-0318 (DG 12 DTEE): DMI's contribution to CEC Final Report Arctic Trophospheric Ozone Chemistry ARCTOC

No. 97-3
Peter Thejll: A search for effects of external events on terrestrial atmospheric pressure: cosmic rays

No. 97-4
Peter Thejll: A search for effects of external events on terrestrial atmospheric pressure: sector boundary crossings

No. 97-5
Knud Lassen: Twentieth century retreat of sea-ice in the Greenland Sea

No. 98-1
Niels Woetman Nielsen, Bjarne Amstrup, Jess U. Jørgensen:
HIRLAM 2.5 parallel tests at DMI: sensitivity to type of schemes for turbulence, moist processes and advection

No. 98-2
Per Høeg, Georg Bergeton Larsen, Hans-Henrik Benzon, Stig Syndergaard, Mette Dahl Mortensen: The GPSOS project
Algorithm functional design and analysis of ionosphere, stratosphere and troposphere observations

No. 98-3
Mette Dahl Mortensen, Per Høeg:
Satellite atmosphere profiling retrieval in a nonlinear troposphere
Previously entitled: Limitations induced by Multipath

No. 98-4
Mette Dahl Mortensen, Per Høeg:
Resolution properties in atmospheric profiling with GPS

No. 98-5
R.S. Gill and M. K. Rosengren
Evaluation of the Radarsat imagery for the operational mapping of sea ice around Greenland in 1997

No. 98-6
R.S. Gill, H.H. Valeur, P. Nielsen and K.Q. Hansen: Using ERS SAR images in the operational mapping of sea ice in the Greenland waters: final report for ESA-ESRIN's: pilot projekt no. PP2.PP2.DK2 and 2nd announcement of opportunity for the exploitation of ERS data projekt No. AO2..DK 102

No. 98-7
Per Høeg et al.: GPS Atmosphere profiling methods and error assessments

No. 98-8
H. Svensmark, N. Woetmann Nielsen and A.M. Sempreviva: Large scale soft and hard turbulent states of the atmosphere

No. 98-9
Philippe Lopez, Eigil Kaas and Annette Guldberg: The full particle-in-cell advection scheme in spherical geometry

No. 98-10
H. Svensmark: Influence of cosmic rays on earth's climate

No. 98-11
Peter Thejll and Henrik Svensmark: Notes on the method of normalized multivariate regression

No. 98-12
K. Lassen: Extent of sea ice in the Greenland Sea 1877-1997: an extension of DMI Scientific Report 97-5

No. 98-13
Niels Larsen, Alberto Adriani and Guido Di-Donfrancesco: Microphysical analysis of polar stratospheric clouds observed by lidar at McMurdo, Antarctica

No.98-14
Mette Dahl Mortensen: The back-propagation method for inversion of radio occultation data

No. 98-15
Xiang-Yu Huang: Variational analysis using spatial filters

No. 99-1
Henrik Feddersen: Project on prediction of climate variations on seasonel to interannual timescales (PROVOST) EU contract ENVA4-CT95-0109: DMI contribution to the final report:Statistical analysis and post-processing of uncoupled PROVOST simulations

No. 99-2
Wilhelm May: A time-slice experiment with the ECHAM4 A-GCM at high resolution: the experimental design and the assessment of climate change as compared to a greenhouse gas experiment with ECHAM4/OPYC at low resolution

No. 99-3
Niels Larsen et al.: European stratospheric monitoring stations in the Artic II: CEC Environment and Climate Programme Contract ENV4-CT95-0136. DMI Contributions to the project

No. 99-4
Alexander Baklanov: Parameterisation of the deposition processes and radioactive decay: a review and some preliminary results with the DERMA model

No. 99-5
Mette Dahl Mortensen: Non-linear high resolution inversion of radio occultation data

No. 99-6
Stig Syndergaard: Retrieval analysis and methodologies in atmospheric limb sounding using the GNSS radio occultation technique

No. 99-7
Jun She, Jacob Woge Nielsen: Operational wave forecasts over the Baltic and North Sea

No. 99-8
Henrik Feddersen: Monthly temperature forecasts for Denmark - statistical or dynamical?

No. 99-9
P. Thejll, K. Lassen: Solar forcing of the Northern hemisphere air temperature: new data

No. 99-10
Torben Stockflet Jørgensen, Aksel Walløe Hansen: Comment on "Variation of cosmic ray flux and global coverage - a missing link in solar-climate relationships" by Henrik Svensmark and Eigil Friis-Christensen

No. 99-11
Mette Dahl Meincke: Inversion methods for atmospheric profiling with GPS occultations

No. 99-12
Benzon, Hans-Henrik; Olsen, Laust: Simulations of current density measurements with a Faraday Current Meter and a magnetometer

No. 00-01
Høeg, P.; Leppelmeier, G: ACE: Atmosphere Climate Experiment: proposers of the mission

No. 00-02
Høeg, P.: FACE-IT: Field-Aligned Current Experiment in the Ionosphere and Thermosphere

No. 00-03
Allan Gross: Surface ozone and tropospheric chemistry with applications to regional air quality modeling. PhD thesis

No. 00-04
Henrik Vedel: Conversion of WGS84 geometric heights to NWP model HIRLAM geopotential heights

No. 00-05
Jérôme Chenevez: Advection experiments with DMI-Hirlam-Tracer

No. 00-06
Niels Larsen: Polar stratospheric clouds microphysical and optical models

No. 00-07
Alix Rasmussen: "Uncertainty of meteorological parameters from DMI-HIRLAM"
(In Press)

No. 00-08
A.L. Morozova: Solar activity and Earth's weather. Effect of the forced atmospheric transparency changes on the troposphere temperature profile studied with atmospheric models

No. 00-09
Niels Larsen, Bjørn M. Knudsen, Michael Gauss, Giovanni Pitari: Effects from high-speed civil traffic aircraft emissions on polar stratospheric clouds

No. 00-10
Søren Andersen: Evaluation of SSM/I sea ice algorithms for use in the SAF on ocean and sea ice, July 2000

No. 00-11
Claus Petersen, Niels Woetmann Nielsen: Diagnosis of visibility in DMI-HIRLAM
(In Press)

No. 00-12
Erik Buch: A monograph on the physical oceanography of the Greenland waters

No. 00-13
M. Steffensen: Stability indices as indicators of lightning and thunder

No. 00-14
Bjarne Amstrup, Kristian S. Mogensen, Xiang-Yu Huang: Use of GPS observations in an optimum interpolation based data assimilation system
(In Press)

No. 00-15
Mads Hvid Nielsen: Dynamisk beskrivelse og hydrografisk klassifikation af den jyske kyststrøm
(In Press)